12-2015

The role of DNA methylation and hydroxymethylation in smooth muscle cell phenotypic change during atherogenesis

jason Williams

THE ROLE OF DNA METHYLATION AND HYDROXYMETHYLATION IN SMOOTH MUSCLE CELL PHENOTYPIC CHANGE DURING ATHEROGENESIS

by

Jason Allen Williams B.A.

APPROVED:

_____
Yong-Jian Geng M.D Ph.D., Advisory Professor

_____
Dr. Mikael Akesson-Wassler Ph.D.

_____
Karen Uray Ph.D.

_____
Jianping Jin Ph.D.

_____
Melvin Klegerman Ph.D.

APPROVED:

_____
Dean, The University of Texas
Graduate School of Biomedical Sciences at Houston

THE ROLE OF DNA METHYLATION AND HYDROXYMETHYLATION IN SMOOTH MUSCLE CELL PHENOTYPIC CHANGE DURING ATHEROGENESIS

A

DISSERTATION

Presented to the Faculty of
The University of Texas
Health Science Center at Houston
and
The University of Texas
MD Anderson Cancer Center
Graduate School of Biomedical Sciences
in Partial Fulfillment

of the Requirements

for the Degree of

DOCTOR OF PHILOSOPHY

Dedication

This work is dedicated to my family and friends who have helped, encouraged, and supported me throughout my education and to all of those who have, and are suffering from disease.

- In loving memory of Kenneth C. Dresser and Robert C. Williams.

Acknowledgments

I would like to express my sincere gratitude to my advisor, Dr. Yong-Jian Geng for his unwavering support, friendship, assistance, and mentorship throughout this project. I would further like to extend my thanks to all those who offered collegial guidance and support throughout the years.

THE ROLE OF DNA METHYLATION AND HYDROXYMETHYLATION IN SMOOTH MUSCLE CELL PHENOTYPIC CHANGE DURING ATHEROGENESIS

Jason Williams, Ph.D.

Advisory Professor: Yong-Jian Geng, M.D Ph.D.

Abstract

Atherosclerosis is a chronic arterial disease which impacts systemically the function of organs and tissues by causing inflammation and disruption of blood supply. During atherogenesis, lipid deposits, inflammation, and cells accumulate within the walls of arteries, ultimately leading to a buildup of fatty plaques and occlusion of the arterial lumen. In a multifactorial disease like atherosclerosis there are complex interplays between environmental, genetic and epigenetic risk factors. The epigenetics of atherosclerosis involving DNA methylation has been progressing from single gene to genome wide analyses. Although these epistudies have provided evidence that DNA methylation exists within certain genes during atherogenesis, the presence and effects of DNA methylation and hydroxymethylation are not fully understood and their impact on vascular cell signal transduction and proliferation may prove to be critically important.

Hypothesis and Aims. The central hypothesis of this project is that an imbalance between DNA methylation and demethylation occurs in the lesions of atherosclerosis, which leads to changes in vascular gene expression, in particular those coding for growth factor receptors. The long term goal of this research is to elucidate the epigenetic mechanisms, mainly DNA methylation and hydroxymethylation, and their contribution to the progression or reprogression of atherogenesis.

The specific aims are to use *in vitro* and *in vivo* models of atherosclerosis to examine the functional role of, and the mechanisms contributing to, DNA methylation and hydroxymethylation in insulin-like growth factor 1 receptor (IGF-1R) expression during atherogenesis triggered by genetic knockout of ApoE and/or the addition of high fat.

Methods and Results. Atherosclerosis is a chronic arterial disease systemically impacting the function of organs and tissues by causing inflammation and disruption of blood supply. The presence and effects of DNA methylation and hydroxymethylation during atherogenesis are not fully understood and their impact on vascular cell signal transduction and proliferation may prove to be critically important. Here we seek to examine the functional role of DNA methylation and hydroxymethylation in insulin-like growth factor 1 receptor (IGF-1R) expression during atherogenesis triggered by genetic knockout of ApoE and/or the addition of high fat. Using cultured vascular smooth muscle cells (VSMCs) and murine models of atherosclerosis, high fat diet feeding augments the inhibitory effect of ApoE

deficiency on DNA methylation and hydroxymethylation in the aortas with severe plaques. Interestingly, the same induction of atherosclerosis causes a decrease in hydroxymethylation but an increase in methylation within the promoter region of the IGF-1R gene. Results detail the identification of TET2 as an epigenetic regulator that acts upstream of IGF-1R during atherogenesis through demethylation of the promoter area. We further show that TET2 mRNA and protein were found to be regulated by the mTORC1 signaling pathway, and selective rapamycin-induced inhibition of mTOR can reactivate IGF-1R expression through up-regulation of TET2 and hydroxymethylation of the IGF-1R promotor.

Conclusion. Identification of altered DNA methylation/hydroxymethylation in the arterial wall during atherosclerosis and its contribution to the down-regulation of IGF-1R during atherosclerosis may lend itself to altering key components of the mTOR-TET2-5-hmC pathway and thereby lead to novel therapeutic targets for treating disease.

Table of Contents

List of Illustrations

Title Page

List of Tables

Abbreviations

4',6-diamidino-2-phenylindole (DAPI)

5-Carboxylcytosine (5caC)

5-Formylcytosine (5fC)

5-hydroxymethylcytosine (5hmC)

5-hydroxymethyluracil (5hmU)

5-methylcytosine (5mC)

American Heart Association (AHA)

Analysis of variance (ANOVA)

Base excision repair (BER)

Body mass index (BMI)

Bovine serum albumin (BSA)

Cardiovascular disease (CVD)

Centers for Disease Control (CDC)

Cytosine base preceded by guanine base (CpG)

Deoxyribonucleic acid (DNA)

Dimethylsulfoxide (DMSO)

DNA methyltransferase (DNMT)

DNA methyltransferase 1 (DNMT1)

DNA methyltransferase 3A (DNMT 3A)

DNA methyltransferase 3B (DNMT 3B)

Endothelial cells (EC)

Enzyme-linked immunosorbent assay (ELISA)

Epidermal growth factor receptor (EGFR)

Fetal bovine serum (FBS)

Glyceraldehyde-3-phosphate dehydrogenase (GAPDH)

Hemotoxilin and eosin (H&E)

High density lipoprotein (HDL)

Horse radish peroxidase (HRP)

Immunoglobulin G (IgG)

Insulin-like growth factor 1 (IGF-1)

Low density lipoprotein (LDL)

Mammalian lethal with SEC13 protein 8 (MLST8)

Mechanistic target of rapamycin complex 1 (mTORC1)

Mechanistic target of rapamycin complex 2 (mTORC2)

Methyl group (CH-3)(m)

Methyl-CpG-binding domain (MBD)

Micro-ribonucleic acids (miRNAs)

Mitogen-activated protein kinase (MAPK)

Natural killer T cells (NKT)

Phosphate buffered saline (PBS)

Phosphoinositide 3-kinase (PI3K)

Polyvinylidene difluoride (PVDF)

Protein kinase B (AKT)

Protein kinase C α (PKCα)

Quantitative polymerase chain reaction (qPCR)

Rapamycin-insensitive companion of mTOR (RICTOR)

Receptor insulin-like growth factor 1 receptor (IGF-1R)

Regulatory-associated protein of mTOR (Raptor)

Reverse transcription quantitative polymerase chain reaction (RT-qPCR)

Ribonucleic acid (RNA)

Room temperature (RT)

Sodium dodecyl sulfate polyacrylamide gel electrophoresis

Ten-eleven translocation 1 (TET1)

Ten-eleven translocation 2 (TET2)

Ten-eleven translocation 3 (TET3)

T-helper 1 cells (T(h)1)

Vascular smooth muscle cell (VSMC)

Chapter 1: Introduction

Motivation for Atherosclerosis Research

Cardiovascular disease (CVD) is a complex multifactorial designation for disorders of the heart and vascular system consisting of heart disease, stroke, other vascular diseases. According to recent data from the Centers for Disease Control (CDC), CVD is the leading cause of death within the United States, accounting for roughly 1 in every 3 deaths annually. An estimated 85.6 million adults suffer from CVD in the United States according to the 2015 statistic from the American Heart Association (AHA) (Mozaffarian, Benjamin et al. 2015). Moreover, CVD is the leading cause of death globally resulting in 17.3 million deaths or 32% in 2014 and becoming more and more prevalent in developing countries (2015).

As the prevalence continues to increase throughout the world, CVD rates are slowly declining within the United States. For instance, from 2001 to 2011, death rates attributable to CVD declined 30.8% and the actual number of CVD deaths per year declined by 15.5%. Although significant progress is being made to decrease the rate and overall deaths, in 2011, CVD still accounted for 31.3% (786,641) of all 2,515,458 deaths, or approximately 1 of every 3 deaths in the United States. On the basis of the 2011 death rate data, more than 2,150 Americans die of CVD each day, an average of 1 death every 40 seconds. Approximately 155,000 Americans who died of CVD in 2011 were younger than 65 years of

age and 34% of deaths attributable to CVD occurred before the age of 75 years, which is younger than the current average life expectancy of 78.7 years (Mozaffarian, Benjamin et al. 2015).

Along with the mortality caused by CVD, the morbidity associated with CVD can have a profound impact not only on a person's capacity to do their job, but also, their capability to work at all. Because of the nature of the disease and the symptoms related to it, the complete economic cost associated with the loss of work due to CVD is difficult to calculate. However, it is estimated that the total occupational and economic cost from CVD, including heart disease, stroke, and high blood pressure, accounts for more economic loss than any other disability, disease, or injury (Price 2004).

As the current statistics show, although progress is being made to decrease the death rate and overall mortality and morbidity, CVD and its underlying conditions remain the most significant disease challenge faced today. That being said, improved prognoses can be attributed, in part, to new therapies and interventions, as well as a better understating of the basic science underlying the disease.

Overview of Atherosclerosis

The underlying mechanisms of CVD vary depending on the subtype of disease, but a atherosclerosis is a major contributing factor. Atherosclerosis is a systemic disease process in which lipid deposits, inflammation, cells, and scar tissue build up within the walls of arteries, ultimately leading to a buildup of fatty plaques and occlusion of the arterial wall. This accumulation and occlusion, as well as the rupture and dislocation of the plaques,

contributes to a large number of cardiovascular incidents. Atherosclerosis is a systemic disease and blood vessels susceptible to atherosclerosis supply the heart, kidneys, brain, as well as every other organ in the body. However, the degree and susceptibility of atherosclerosis varies between patients and may produce different effects in the size of the plaque area and the vessels and locations.

Cellular Components of Atherosclerosis

Atherosclerosis is a disease originating within arteries. The arteries are vessels primarily responsible for the transportation of blood from the heart throughout the circulatory system. The artery is a tubular structure consisting of three distinct layers, the tunica adventitia or externa, tunica media, and tunica intima, which are separated by an internal and external elastic membrane. The layer closest to the lumen of the artery is the tunica intima which contains a single layer of endothelial cells (EC) arranged in a cobblestone-like morphology. ECs line the vessel and are involved in several functions as they come in contact with blood, such as, providing an anti-thrombogeneic effect, hormone, nutrient, and cytokine trafficking, and neutrophil recruitment. The tunica media, separated from the tunica intima by layers of elastin, makes up the majority of the artery and consists primarily of vascular smooth muscle cells (VSMC). VSMCs are arranged in concentric layers of cells interlaced with a matrix consisting of collagen, elastin, and proteoglycans. VSMCs contain three types of adrenergic receptors, α_1,α_2, and β_2. These receptors act to regulate muscle tone and provide a vascular response to various stimuli within the artery through vasoconstriction and dilation. Surrounding the tunica

media and separated by a external elastic membrane is the tunica adventitia. The tunica adventitia consists of a loose connective tissue layer containing collagen and permeated with by blood vessels. These blood vessels, named vasa vasorum, serve to provide nutrients and oxygen to the metabolically active medial layer. As the arteries progress further from the heart, they bifurcate and branch out, forming progressively smaller vessels with smaller, less dense, tunica medial layers as they progress from arterioles to capillaries.

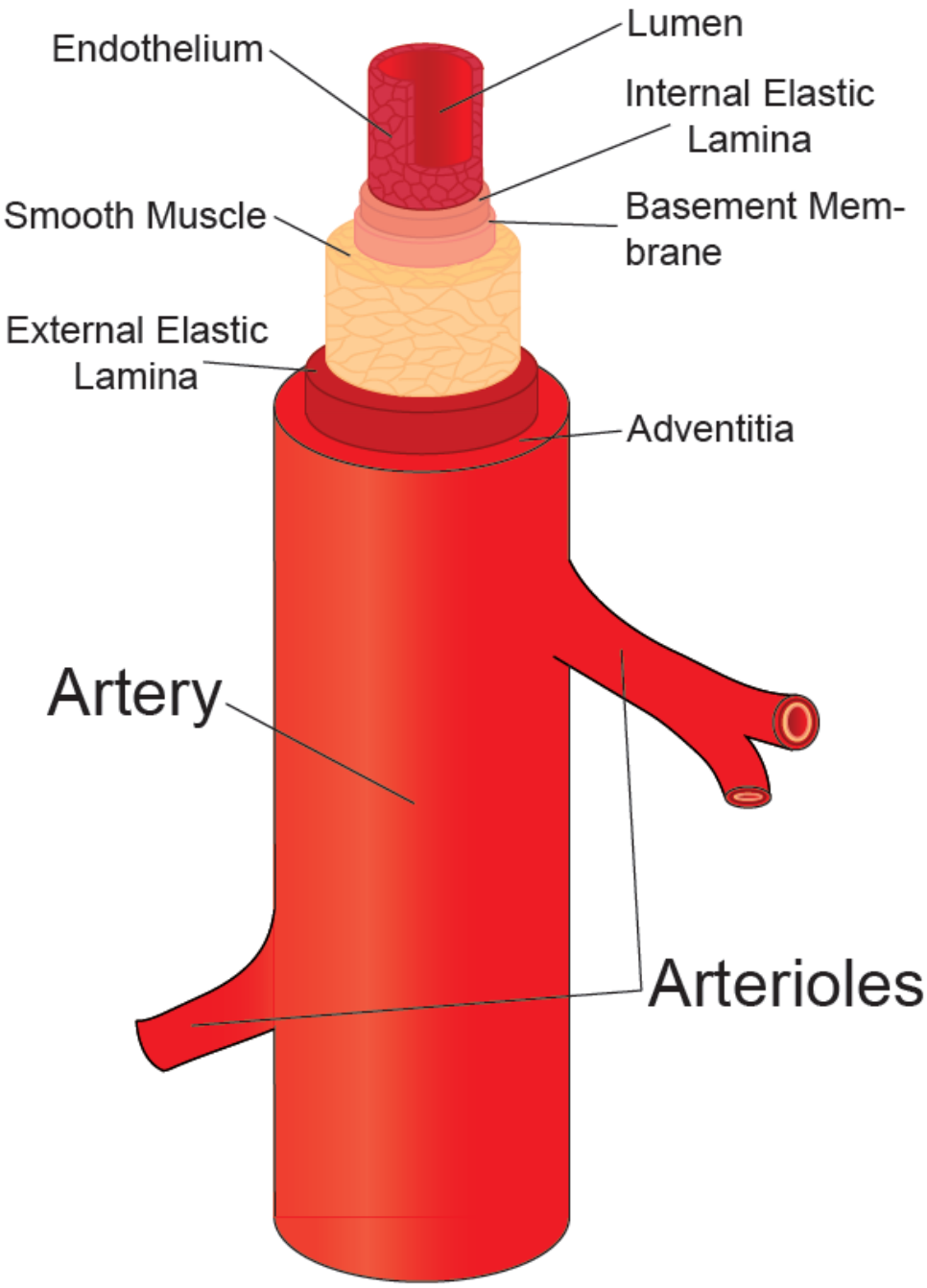

Figure 1. Gross anatomical structure of the artery.

Diagram of a large artery and the major contributing layers. The artery consists of three main layers, the adventitia, media, and intima, and their contributing cellular and non-cellular components.

Pathogenesis of Atherosclerosis

Atherosclerosis is the thickening of the arterial wall in a process caused by inflammation, cellular migration and cellular dysfunction. The formation of atherosclerosis begins with an initial lesion, which, although morphologically "normal", is characterized by macrophage infiltration and isolated foam cells, which are macrophages laden with low-density lipoproteins (LDLs), as well as other lipids. As the lesion progresses, the formation of a fatty streak arises, which is distinguished by greater numbers of foam cells beneath the endothelium and by intracellular lipid accumulation (Rader and Daugherty 2008).

As atherosclerosis progresses, an intermediate lesion followed by an atheroma is formed. This process is marked by greater intracellular lipid accumulation and extracellular lipid pooling, as well as VSMCs infiltrating and proliferating within the lesion. VSMCs produce extracellular matrices made up primarily of collagen, which leads to greater amounts of extracellular lipid pooling and the formation of extracellular lipid cores. As the atheroma develops, chronic inflammation drives an immune response which leads to recruitment of T cells to the atherosclerotic plaque. During the transition from atheroma to a fibroatheroma, VSMCs continue to increase and a fibrous cap is formed through the entrapment of cholesterol and other cellular debris in and around the endothelial cell layer. It is also during this time that lipid cores accumulate and cells become necrotic, releasing crystalline cholesterol that can lead to calcification. As this occurs, atherosclerosis transitions from clinically silent to clinically overt and contributes to clinical symptoms of atherosclerosis. When surface deficits become present within the fibrotic cap, the plaque becomes a complicated lesion. This type of plaque tissue can completely occlude vessels and, due to surface deficits and instability, is rupture prone which can cause thromboses and ultimately lead to stroke or MI.

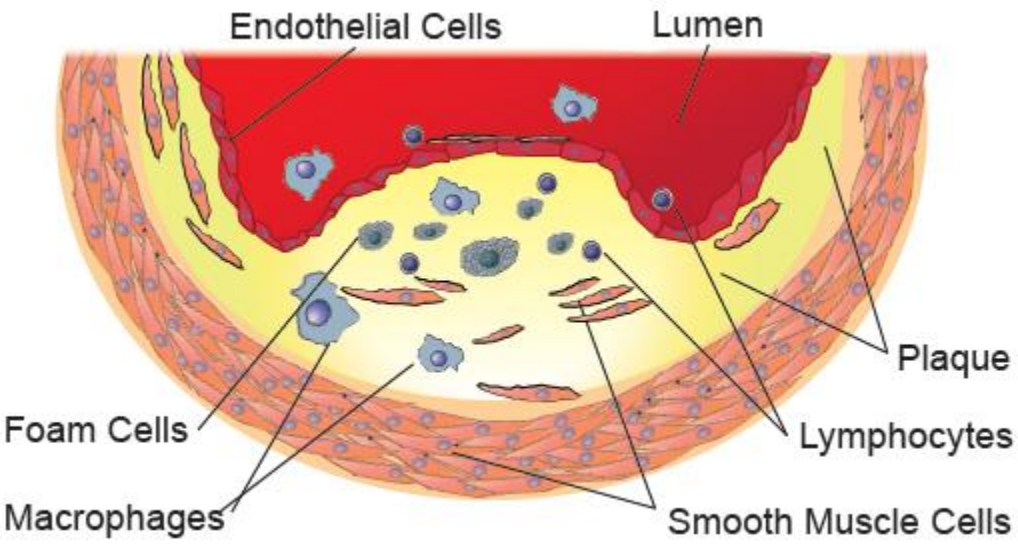

Figure 2. Cellular components of an atherosclerotic plaque.

During the process of atherogenesis, plaque tissue is marked by cellular migration and dysfunction triggered by inflammation. Cellular recruitment of lymphocytes, specifically CD4+ T helper 1 (Th1) and natural killer T (NKT) cells, occurs as an immune response and to clear glycolipid antigens. Migration of macrophages within the plaque to clear cellular debris and lipid accumulation creates pro-atherogenic foam cells. As the severity of the plaque progresses, migration and proliferation of VSMC causes medial thickening. During late stages, the plaque undergoes endothelial damage and dysfunction, causing the formation of a fibrous cap, which ultimately, leads to instability and plaque rupture.

Complications from Atherosclerosis

The process of atherosclerosis progression typically occurs over a decades-long period of time. During the early stages of atherosclerosis, the effects are often clinically silent. Nevertheless, as the endothelium erodes and becomes damaged, there is the possibility that the formation of thrombi can occur quickly. This sudden formation of a thrombus often results in the total occlusion of the vessel. However, more frequently the endothelium will remain intact, causing the artery to compensate as the atherosclerotic plaque transitions from an intermediate lesion to an atheroma. As this occurs, the artery can dilate and maintain the approximate luminal dimensions until the atheroma reaches around 35-40% occlusion. At this time the lumen will become increasingly narrow, impeding the blood flow rate and frequently, as a compensatory mechanism, elevating blood pressure. The atherosclerotic plaque typically does not enlarge at a constant rate, but rather in short segments. This may be accounted for by the disruption of micro-vessels that supply nutrients to the VSMCs within the tunica media.

As these vessels become damaged due to inflammation, they can cause intra-plaque hemorrhage, which in turn, can stimulate VSMC recruitment and proliferation (Dutta, Courties et al. 2012). During this process, where arterial occlusion worsens, the clinical manifestations change from clinically silent to overt and include a host of complications, including unstable angina pectoris, peripheral artery disease, and ischemic stroke. As the fibrous cap of a complicated lesion ruptures, this results in the release of inflammatory cytokines and coagulation factors into the circulating blood and around the

proximity of the plaque. The result is rapid clot formation that has been shown to account for roughly 75% of acute myocardial infarctions (Libby 2002).

Risk Factors

During the late 1940's, scientists and a group of recruited patients embarked on an ambitious project to identify contributing causes of cardiovascular disease in what was termed the Framingham Study (Dawber, Meadors et al. 1951). The term "risk factor" was introduced into medical terminology during the course of the study to describe the causes of pathophysiological events; the modifications of which could significantly decrease the likelihood of adverse cardiovascular and cerebrovascular events (Dawber, Kannel et al. 1959). Since the Framinham Study, many more studies have been conducted to illuminate all apsects of the adverse affects of risk factors for CVD and to discover new ways to treat them and improve prognosis. Numerous risk factors exist for atherosclerosis, including anatomical and physiological factors which can be subdivided into various categories such as congenital and acquired, modifiable or not, etc. While too numerous to list in their entirety, perhaps the most useful of these are those termed classical risk factors. They include some of the highest contributors to atherosclerosis, including hypertension, smoking, diet and obesity, high blood cholesterol, and diabetes.

Hypertension

Hypertension occurs when the blood pressure in the arteries is elevated and is defined as a systolic pressure greater than 140 mm Hg and/or a diastolic pressure greater than 90 mm Hg. Hypertension is associated with abnormal structural and functional changes in the vascular wall and affects more than 77.9 million people in the United States (Go, Mozaffarian et al. 2014). Many mechanisms have been proposed to account for the pathogenesis, but generally they include endothelial injury and/or dysfunction, hemodynamic factors, cell membrane (ion transport and receptor) abnormalities, proliferation and growth of vascular cells, vasoactive substances, platelet dysfunction, and lipoprotein deposition and clearance (Dzau 1988). The structural and functional changes in the vasculature resulting from hypertension are both caused by and can accelerate the development of atherosclerosis.

High Blood Cholesterol

Cholesterol and triglycerides are transported throughout the bloodstream bound within proteins called lipoproteins. Cholesterol is transported as two major types of lipoproteins; low density lipoproteins (LDL) and high density lipoproteins (HDL). Both forms of lipoprotein have significant impacts on atherosclerosis. LDL and its subclasses of lipoproteins transfers lipids and cholesterol throughout the circulation, which in turn are taken up by cells by receptor mediated endocytosis. This process exacerbates atherosclerosis when LDLs are taken up by ECs and other cells within the artery, which can then become

oxidized by necrotic cell debris and free radicals (Selwyn, Kinlay et al. 1997). Conversely, HDL transports cholesterol and lipids back to the liver for removal from the circulation. Blood cholesterol is considered high if the total blood cholesterol concentration is above 240 mg/dl and/or the ratio of LDL to HDL is greater than 3:1. High blood cholesterol can be caused by several factors, including both genetic and environmental. Genetic or familial hypercholesterolemia is caused by a genetic defect on chromosome 19 and is inherited by family members in an autosomal dominant manner. This condition causes an accumulation of LDL within the bloodstream due to an inability of the body to remove cholesterol. The condition begins at birth and can cause cardiovascular dysfunction and atherosclerosis at a young age. In addition to genetic defects, environmental factors such as diet, weight, and physical activity contribute to hypercholesterolemia and CVD.

Diet and Obesity

Major risk factors for CVD and atherosclerosis are diet and body mass. Foods such as animal products, including meat, cheese, and egg yolks, as well as processed foods and those containing saturated and *trans* fatty acids contain fats which can elevate blood lipid and cholesterol levels and lead to weight gain. All other factors being equal, individuals who are overweight or obese have a positive correlation with higher LDL levels, lower HDL levels, and higher total cholesterol levels, all of which are risk factors and contribute to CVD and atherosclerosis.

Models of Atherosclerosis

A wide array of models which mimic aspects of atherosclerosis have been utilized to better understand certain characteristics involved in the pathophysiology of the disease and include animal, lower organism, genetic, *in silico*, analytical, and kinetic models (Singh, Tiwari et al. 2009). Among the most commonly used are cellular and animal models which throughout the years have provided valuable insight. However, due to the complex and multifactoral nature of the disease, no model perfectly replicates human atherosclerosis and each model has inherent limitations. Ultimately, any useful disease model should contain several aspects, including availability, affordability of establishment and maintenance, ease of manipulation, and, most importantly, a close similarity to human disease.

Cellular Models of Atherosclerosis

Cellular models provide the basis for much of biomedical research currently being conducted. Their advantages are their accessibility, affordability, and their ease of manipulation. Additionally, cellular models, with the possible exception of human embryonic stem cells, carry none of the ethical concerns associated with genetic manipulation and drug testing that are seen in animal models. The ability to easily and efficiently over-express, knock-down, and silence genes provides a valuable tool for drug testing and discovery, as well as to investigate contributing pathophysiological mechanisms and pathways. However, because of the multicellular nature of atherosclerosis, no cell-based model faithfully recreates the complex environment or natural progression of the disease.

Cell-based models utilize all cellular components, such as T-cells, NKT cells, macrophages and endothelial cells. These cells can be both cultured or freshly isolated from human and animal models. However, the most utilized model is VSMCs, which comprise the majority of the cellular content within the artery and atherosclerotic lesion. With respect to all cellular models, it is important to remember that aspects of what occurs within *in vitro* models of atherosclerosis are not always representational or predictive of what occurs within *in vivo* disease states.

Animal Models of Atherosclerosis

Numerous animal models exist and have been used in the study of the pathophysiology of human atherosclerosis. These models range from large animals such as rabbits, pigs, and non-human primates to smaller animals such as fish, rats, and mice. While no animal model is perfectly identical to human atherosclerosis, each model has its own intrinsic advantages and limitations as it pertains to modeling the initial atherogenesis, atherosclerotic progression and regression, and manipulation of lipid profiles. Currently, one of the most commonly used animal models, due in large part to the ease of genetic manipulation and relatively short time period to induce atherosclerotic lesions, is the mouse model. The induction of atherosclerosis in murine models of the disease is accomplished in two main ways, manipulation of a diet and genetic knockout. Although murine models do not naturally develop atherosclerosis on a normal chow, diet induction of atherosclerosis can be accomplished with adjustments to calories and fat content. However, not all murine strains are equally prone to atherosclerosis while some strains are resistant, the C57BL/6J

strain is the most susceptible to atherosclerosis when fed an atherogenic high fat, high cholesterol, or cholic acid containing diet (Paigen, Morrow et al. 1987).

Alternatively, the induction of atherosclerosis can be achieved through genetic manipulation of the model. Several genes have been identified as having a critical role in the transport and metabolism of lipids and providing athero-protective benefits. The genetic knockout of genes can cause induction of atherosclerosis without the need for adjustments to diet. Two such genes are LDL receptor and apoliporotein E (ApoE), The genetic knockout of these genes provides two of the most frequently used models in atherosclerosis research.

ApoE Knockout Murine Model of Atherosclerosis

Of the murine models of atherosclerosis, one the most frequently used models is the ApoE knockout model (Plump, Smith et al. 1992). ApoE is a 34kDa lipoprotein that is secreted in various cells, such as macrophages, VSMCs and myoblasts, as well as other cells in numerous organs such as the liver, lungs, kidneys, and spleen (Beisiegel, Weber et al. 1988; Koo, Wernette-Hammond et al. 1988). ApoE is a major lipoprotein that exists in humans as 3 isoforms, v2, v3, and v4, with ApoE v3 being the most common. ApoE acts as a scavenger and transporter of lipids, cholesterol and other associated proteins. Upon binding, lipids and cholesterol are transported to the liver for metabolism and further processing (Cedazo-Minguez 2007). In the murine genetic knockout model of ApoE, the ApoE gene is excised in a C57BL/6J background, resulting in a strain that spontaneously develops and exhibits all stages of atherosclerosis. ApoE knockout mice display a

cholesterol level in excess of four times greater than C57BL/6J and this difference can be further exacerbated by the addition of a calorie and fat adjusted diet (Zadelaar, Kleemann et al. 2007).

Epigenetics

Epigenetics seeks to describe active alterations in the transcriptional potentiality of a cell through the modification of gene expression rather than alteration of the genetic code itself (Holliday 1994). Differing from genetics, where changes are based solely on the deoxyribonucleic acid (DNA) sequence, the changes in gene expression and cellular phenotype associated with epigenetics are due to other causes, primarily modifications of DNA, such as methylation and hydroxymethylation of cytosine, covalent modification of histones through acetylation, methylation, phosphorylation, ubiquitination, and sumoylation and modification with micro-ribonucleic acids (miRNAs), as well as other members of non-coding ribonucleic acids (RNAs). Genetics alone cannot account for many diseases' wide plethora of transcriptional and phenotypic changes. In this study, we focus on epigenetic covalent modifications to DNA in which the prevalence and genomic distribution varies widely. This variability may suggest that there are distinct modes of targeting and function within atherosclerosis.

DNA Methylation and Hydroxymethylation

The process of methylation allows for a mechanistic way to reversibly create a molecular mark on genomic DNA via the addition of a methyl ($C\text{-}H_3$) group (Schubeler 2015). Although bacteria can methylate both adenine and cytosine for processes such as tracking mismatched nucleotide repairs or identifying foreign DNA (Arber and Dussoix 1962; Wion and Casadesus 2006), in eukaryotic cells, methylation only occurs on cytosine residues.

The discovery that the microinjection of methylated DNA at highly specific sites into the nuclei of *Xenopus laevis* oocytes causes transcriptional inactivation suggested a eukaryotic function for DNA methylation (Vardimon, Kressmann et al. 1982). The mechanism was later confirmed in cultured mammalian cells with the *in vitro* methylation of the hamster adenine phosphoribosyltransferase gene inhibiting its expression in mouse cells (Stein, Razin et al. 1982). These and numerous subsequent studies showed that the expression of certain genes may be inhibited by site-specific methylation, functionally linking DNA methylation to gene repression.

In mammalian somatic cells, methylation primarily occurs when cytosine is followed by guanine (CpG), often arranged in clusters called CpG islands that are present in the 5' regulatory regions of many genes. Although DNA methylation normally occurs and performs its regulatory functions in CpG sites and CpG islands, non-CpG methylation is prevalent in embryonic stem cells (Ramsahoye, Biniszkiewicz et al. 2000). The sequence symmetry of the CpG pairing allows for the heritability of DNA methylation at that dinucleotide through cell division. This heritability enables stable epigenetic repression in

genomic imprinting, X-chromosome inactivation, and suppression of repetitive elements (Jones 2012). In vertebrates, DNA methylation is widespread, with between 60% and 90% of CpG sites being methylated in mammals, depending on the tissue, suggesting it may be a default state (Ehrlich, Gama-Sosa et al. 1982). DNA methylation is traditionally removed early on in the formation of the zygote and then later on it is reestablished through consecutive cell divisions during early development.

The mechanism responsible for DNA methylation involves the addition of a methyl group to the 5' carbon of a cytosine base by various enzymes termed DNA methyltransferases (DNMTs), which can be grouped into two general classes of enzymatic activities; maintenance methylation and *de novo* methylation. Maintenance methylation is the process in which the established DNA methylation patterns are copied to the daughter strands during DNA replication. DNMT1 is needed in S phase to methylate newly replicated CpGs occurring opposite methylated ones on the mother strand of the DNA and is recruited by associated methyl-CpG-binding domain proteins (Kimura and Shiota 2003; Sharif, Muto et al. 2007). On the other hand, de novo methylation, carried out by DNMT3A and DNMT3B in combination with DNMT3L, establishes patterns of methylation, predominantly during gametogenesis and development, that lead to cellular differentiation (Okano, Bell et al. 1999; Hata, Okano et al. 2002).

Mechanistically there are two ways in which DNA methylation silences gene transcription. The methyl (CH_3) group can regulate gene expression by modulating and physically impeding the interaction between DNA and transcription factors such as RNA polymerase, enhancers, and activator proteins (Choy, Movassagh et al. 2010). Possibility

more importantly, DNA methylation can repress transcriptional activity through the recruitment and binding of methyl-CpG-binding domain (MBD) proteins such as Methyl-CpG-Binding Protein 2 (Nan, Meehan et al. 1993). These MBDs can then bind additional proteins, such as histone deacetylases and various other chromatin remodeling proteins which, in turn, modify histones, thereby modifying and inactivating chromatin through the formation of heterochromatin (Nan, Ng et al. 1998).

The removal of methylated cytosine bases occurs in two separate ways; passive and active demethylation. Passive demethylation occurs when there is a failure of maintenance methylation, carried out by DNMT1 in S phase, to methylate newly replicated daughter strands during DNA replication (Hsieh 1999). Secondly, passive demethylation can occur due to cytosine's spontaneous deamination to thymine, which occurs frequently in both methylated and non-methylated cytosines throughout the genome (Chen, Ueda et al. 2003). In this case the thymine residue is recognized for the thymine/guanosine mismatch, removed and repaired through normal base excision repair mechanisms.

On the other hand, and functionally more important, is active demethylation in which removal carried out through oxidation is the best documented. The oxidation of the methyl group in 5-methylcytosine (5mC) leads to its conversion to 5-hydroxymethylcytosine (5hmC), an alternate DNA pyrimidine nitrogen base. The ten-eleven translocation (TET) family of proteins are a group of 2-oxoglutarate (2OG)- and Fe(II)-dependent enzymes that catalyzes conversion of 5mC to 5hmC (Tahiliani, Koh et al. 2009). The exact function of 5hmC is still not fully elucidated, but numerous studies have shown it can activate gene

expression and lead to further modifications of the base to convert it back to cytosine. 5hmC can be either deaminated by Activation-induced cytidine deaminase (AID) /Apobec enzymes to give 5-Hydroxymethyluracil (5hmU) (Guo, Su et al. 2011) or it can be further oxidized by TET enzymes to 5-Formylcytosine (5fC) and 5-Carboxylcytosine (5caC) and converted back to cytosine (Globisch, Munzel et al. 2010; He, Li et al. 2011).

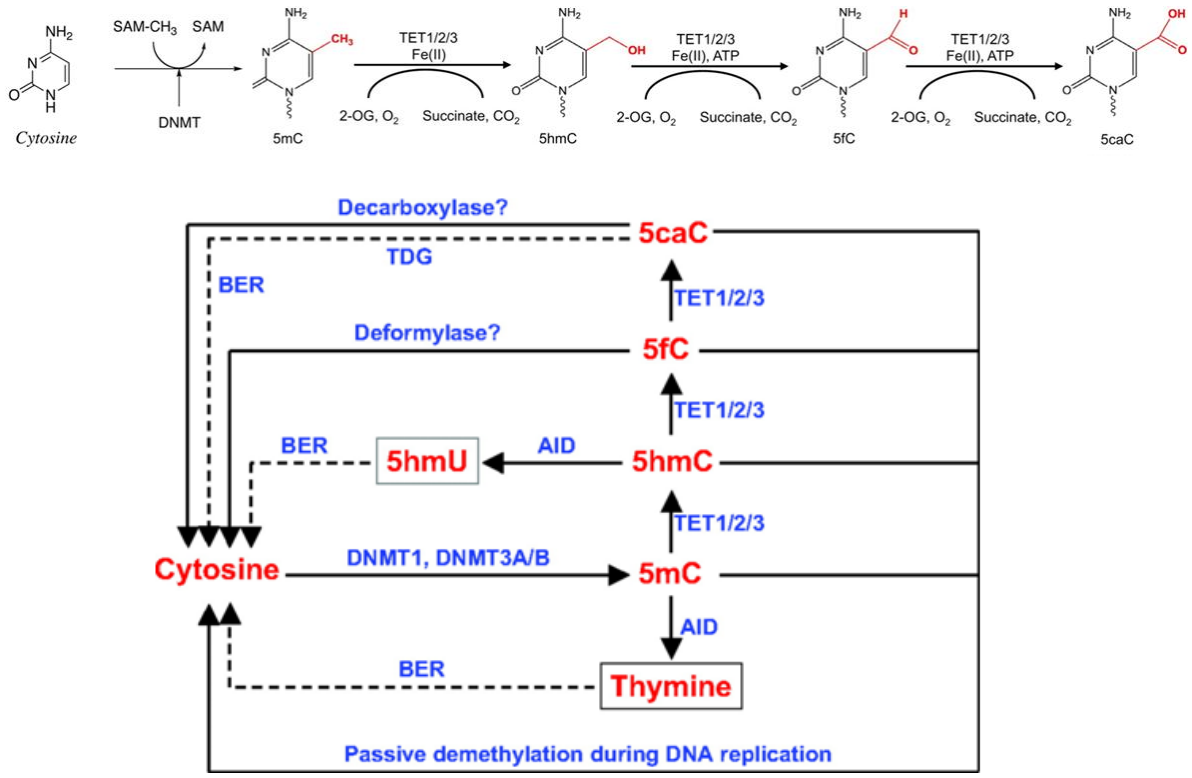

Figure 3. Epigenetic modifications of cytosine

Epigenetically important modification to cytosine center around the addition to, and modification of, the 5' carbon of cytosine. Cytosine can be converted by DNA methyl-transferases (DNMTs) to form 5-methycytosine (5mC). 5mC can either be converted to thymine and converted back to cytosine through base excision repair (BER) or converted to 5-hydroxymethylcytosine (5hmC) by ten-eleven translocation (TET) enzymes. 5hmC can be either deaminated by AID /Apobec enzymes to give 5-Hydroxymethyluracil (5hmU) (Guo, Su et al. 2011)or it can be further oxidized by TET enzymes to 5-Formylcytosine (5fC) and 5-Carboxylcytosine (5caC) and converted back to cytosine (Guo, Su et al. 2011) (Globisch, Munzel et al. 2010; He, Li et al. 2011). Finally, all cytosine modification can passively be demethylated during DNA replication.

DNA Methylation in Atherosclerosis

Epigenetic studies into atherosclerosis focusing on DNA methylation date back over 15 years, first focusing on single genes and progressing to genome wide analyses. These studies have provided firm evidence that not only does DNA methylation exist within certain genes but, as in the case of estrogen receptor gene alpha (ER alpha), methylation can greatly affect expression during atherogenesis (Post, Goldschmidt-Clermont et al. 1999).

Several types of cells, including monocytes and lymphocytes have been studied for alterations in the patterns of DNA methylation. These cell types have been studied not only for their contribution to atherosclerosis, but also the ease of attainability. Genome-wide studies have revealed a global hypomethylation and have proposed elevated homocysteine levels, a known risk factor for CVD, as a possible mechanism. High levels of circulating homocysteine has the ability to inhibit DNMT (Castro, Rivera et al. 2003). Aside from DNA methylation, little information is known about the contribution of hydroxymethylation in atherosclerosis.

Mechanistic Target of Rapamycin (mTOR)

Mechanistic target of rapamycin (mTOR) is a serine/threonine protein kinase originally indentified as a mammalian protein targeted by the G1-arresting rapamycin-receptor complex (Brown, Albers et al. 1994). mTOR acts as the catalytic subunit of two structurally distinct complexes: mechanistic target of rapamycin complex 1 (mTORC1) and mechanistic target of rapamycin complex 2 (mTORC2) (Kunz, Henriquez et al. 1993;

Helliwell, Wagner et al. 1994). Both complexes localize to different subcellular compartments, thus affecting their activation and function and have regulatory functions including cell growth, cell proliferation, cell motility, cell survival, protein synthesis, autophagy, and transcription (Hay and Sonenberg 2004).

mTORC1 is composed of mTOR, regulatory-associated protein of mTOR (Raptor), mammalian lethal with SEC13 protein 8 (MLST8) and the non-core components PRAS40 and DEPTOR (Kim, Sarbassov et al. 2002; Kim, Sarbassov et al. 2003). This complex functions as a nutrient/energy/redox sensor and controls protein synthesis The activity of mTORC1 is stimulated by insulin, growth factors, serum, phosphatidic acid, amino acids, and oxidative stress (Fang, Vilella-Bach et al. 2001).

mTOR Complex 2 (mTORC2) is composed of mTOR, rapamycin-insensitive companion of mTOR (RICTOR), MLST8, and mammalian stress-activated protein kinase interacting protein 1 (mSIN1)(Frias, Thoreen et al. 2006). mTORC2 has been shown to function as an important regulator of the cytoskeleton through its stimulation of F-actin stress fibers, paxillin, RhoA, Rac1, Cdc42, and protein kinase C α (PKCα) (Sarbassov, Ali et al. 2004).

Reports over the last few years clearly demonstrates that mTOR exerts its regulatory functions through a very large number of downstream targets, some of which are phosphorylated directly by mTOR, but many are phosphorylated indirectly.

Insulin-like growth factor 1 (IGF-1)

Insulin-like growth factor 1 (IGF-1) is a hormone that shares a similarity in molecular composition to insulin. It plays a critical role in cellular signaling transduction and regulates cell growth, differentiation, apoptosis, transformation and other important physiological processes. Its primary function is acomplished by binding to its specific receptor insulin-like growth factor 1 receptor (IGF-1R), a tyrosine kinase growth factor receptor. IGF-1R mainly engages in the Ras/mitogen-activated protein kinase (MAPK) pathway and also forms cross-talk with the epidermal growth factor receptor (EGFR) pathway. Notably. it engages in the the phosphoinositide 3-kinase/protein kinase B (PI3K/AKT) pathway and its downstream partner, mTOR. In cardiovascular diseases, evidence suggests it may regulate contractility, metabolism, hypertrophy, apoptosis, autophagy, stem cell regeneration and senescence (Ren and Anversa 2015).

Chapter 2: Hypothesis and Aims

Rationale

Epigenetics play an important role in vascular biology and disease. Studies of epigenetic profiles in atherosclerosis have been focused on DNA methylation and date back over 15 years, analyzing from single gene modifications to genome wide DNA methylation profiles. These studies have provided firm evidence that not only does DNA methylation exist within certain genes but, as in the case of estrogen receptor gene alpha (ER alpha), methylation can greatly affect expression during atherogenesis (Post, Goldschmidt-Clermont et al. 1999). The majority of these studies have utilized bisulfite conversion of methylated DNA, which although valuable cannot distinguish between DNA methylation and hydroxymethylation marks. Bisulfite conversion, also known as bisulfite treatment, is a molecular process which deaminates unmethylated cytosine bases to produce uracil in DNA. Bisulfite conversion is largely considered to be the "gold standard" to test numerous downstream applications assessing the methylation status of DNA. Methylated or hydroxymethylated cytosines bases are protected from the conversion to uracil, allowing the use of other applications to determine the locations and frequencies of unconverted cytosines at a single-nucleotide resolution (Frommer, McDonald et al. 1992). Although this has long been the "gold standard" the inability to differentiate methylation and hydroxymethylation is an important consideration because the functional consequences of these two modifications are very different. Therefore, to determine what contribution is

made by DNA hydroxymethylation tools that can accurately differentiate both modifications should be utilized.

The long term goal of this research is to elucidate the contribution of the epigenetic mechanisms of DNA methylation and hydroxymethylation to the pathophysiological process of vascular cell differentiation during atherogenesis.

Hypothesis

Abnormal epigenetic regulation of vascular cell gene expression contributes to the pathogenesis of atherosclerosis in the arterial wall exposed to environmental risk factors, such as hypercholestolemia and hypertension, by up-regulating harmful genes and down-regulating protective genes. These aberrant expression patterns will lead to a differentiation from a contractile to synthetic phenotype and the exacerbation of atherosclerosis. Therefore the specific aims of these studies are:

Specific Aims

Aim 1:

To determine the contribution of DNA methylation and hydroxymethylation to the epigenome of vascular smooth muscle cells during the process of atherogenesis.

1.1) To create an *in vivo* mouse model representative of the stages of the complex multifactorial nature of atherosclerosis.

1.2) To determine the genome-wide epigenomic contribution of DNA methylation and hydroxymethylation and their relative ratios to diseased and healthy states in the murine atherosclerosis model.

1.3) To determine the locus specific DNA methylation and hydroxymethylation alterations during the process of atherogenesis and identify specific genes affected.

Aim 2:

To determine the mechanisms that impact the relative amounts and contributions of DNA methylation and hydroxymethylation in the epigenome of vascular smooth muscle cells during the process of atherogenesis.

2.1) To determine which members of TET family of DNA hydroxylases are involved in the conversion of DNA methylation to hydroxymethylation and subsequent gene activation during the process of atherogenesis.

2.2) To determine the mechanism by which the involved TET enzymes are regulated in atherogenesis and to test whether the pathway promotes the contractile VSMC to dedifferentiate to a synthetic phenotype by altering DNA methylation/hydroxymethylation.

Chapter 3: Materials and Methods

Murine Models of Atherosclerosis

Atherosclerosis-prone ApoE knockout and C57BL/6J Wild Type mice (male, 3 months old) were obtained commercially from Jackson Laboratory and were housed in a climate-controlled environment (Plump, Smith et al. 1992). Mice were fed for a period of 15 weeks with either normal chow (TD.05230 Mouse/Rat Sterilizable Diet, containing 6.2% kcal from fat) or a western diet (TD.88137 Mouse/Rat Adjusted Calories Diet, containing 47% kcal from fat) (Teklad Lab Animal Diets, Harland Laboratories). All experimental procedures and protocols used in this investigation were reviewed and approved by the Institutional Animal Care and Use Committee of The University of Texas Health Science Center at Houston.

Determination of Body Weight/Body Mass Index

Mice were anesthetized with a 2% isoflurane/oxygen mixture using a VetFlo Rodent Anesthesia Vaporizer (Kent Scientific) and weighed using a digital centigram balance (Intell-Lab). Body mass index was calculated using average body length measured from the tip of the snout to the anus and using the following formula:

$$BMI = \text{Body Weight (kg)}/\text{Body Length (meter)}^2$$

Analysis of Blood Pressure

Mice were placed in plastic restrainers and, when the animals relaxed, a volume pressure recorder cuff was gently attached to the tail. Mice were allowed to habituate to this procedure for 7 days prior to the experiments being performed. Systolic and diastolic blood pressure values were recorded on a CODA-HT8 (Kent Scientific) and were averaged from ten consecutive readings obtained from each mouse. Mean arterial pressure was calculated using the formula (MAP = [(2x diastolic)+systolic]/3).

Collection of Blood Samples

Blood collection was done under general anesthesia with a 2% isoflurane/oxygen mixture using a VetFlo Rodent Anesthesia Vaporizer (Kent Scientific). Using heparinized micro-hematocrit capillary tubes (Fisherbrand), 200 ul of whole peripheral blood was collected from the medial canthus via retro-orbital puncture of the sinus membrane. Blood serum was separated with an Eppendorf 5424 centrifuge at 2,000 x g for 10 minutes. Lipid profile containing HDL, VLDL, LDL, Triglycerides, and Cholesterol was analyzed (Equine Laboratories).

Ultrasound Assessment

Echocardiography was performed under anesthesia with a 2% isoflurane/oxygen mixture using a VetFlo Rodent Anesthesia Vaporizer (Kent Scientific). Mice were placed on

a rodent warming pad and extremities were fixed by gently placing the mouse in a supine position. Precordial areas were cleaned by pre-warmed hair removal gel (Nair) left on skin briefly for 1-2 minutes. Echocardiography was performed using Vevo 2100 ultrasound machine and Visualsonics software (FUJIFILM VisualSonics, Inc). The following echocardiographic and transthoracic aortic parameters were recorded with a RMV 704 (Real-Time Micro Visualization) scanhead with traducer frequency at 50 MHz in B and M-Modes: Heart rate, left ventricular (LV) diameters (systolic and diastolic, s/d), LV ejection fraction, fractional shortening, LV wall thickness, LV wall motion abnormalities (defined as basal and apical-mid segments), and aortic intimal thickness.

Collection of Aortic Tissue

Mice were anesthetized with a 2% isoflurane/oxygen mixture using a VetFlo Rodent Anesthesia Vaporizer (Kent Scientific) and were euthanized by cervical dislocation. Whole aortic tissues were excised starting at the aortic valve to the abdominal aorta approximately 8 mm prior to the iliac bifurcation. Aortic tissue was processed for extraction of DNA, RNA, proteins, and preparation for sectioning.

Isolation of Genomic DNA

Total DNA was obtained from cell cultures and aortic arch tissue approximately 5 mm from the outlet of the aortic valve. Aortic tissue was manually separated removing adventitial connective tissue and endothelium. Medial tissue was then incubated for 10 min

at 37^{o} C with collagenase type II (Worthington Laboratories) and resulting cells were subjected to further processing. Extraction was done using DNeasy column collection kit (QIAGEN) per manufacturer's instructions. Extracted DNA was quantified with a DU 730 UV/Vis Spectrophotometer (Beckman Coulter) and was stored at -80^{o} C.

Isolation of RNA

Total RNA was obtained from cell cultures and aortic arch tissue approximately 5mm from the aortic valve. Aortic tissue was manually separated removing adventitial connective tissue and endothelium. Medial tissue was then incubated for 10 min at 37^{o} C with collagenase type II (Worthington Laboratories) and resulting cells were subjected to further processing. Extraction was done using TRIzol reagent (Invitrogen) and purified with RNeasy Plus RNA preparation kit (QIAGEN)) per manufacturer's instructions. Extracted RNA was quantified using a DU 730 UV/Vis Spectrophotometer (Beckman Coulter) and was stored at -80^{o} C.

Protein Extraction

Protein was extracted from cell cultures and aortic arch tissue approximately 5 mm from the aortic valve. Aortic tissue was manually separated removing adventitial connective tissue and endothelium. Medial tissue was then incubated for 10 min at 37^{o} C with collagenase type II (Worthington Laboratories) and resulting cells were lysed in solubilisation buffer (50 mM HEPES, pH 7.5; 150mM NaCl; 1mM EGTA; 20mM_-

glycerophosphate; 1% Nonidet P-40; 10 mM NaF; 2 mM Na3VO4; and protease inhibitors). Protein fractions were separated with a 5424 centrifuge (Eppendorf) at 2,000 x g for 10 minutes and stored at -80^{o} C.

Isolation and Culture of VSMC

VSMC were isolated and cultured from the aortic tissues of Wild Type and ApoE-/- mice (male, 6 months old). After removing adventitial connective tissue and endothelium, medial muscle cells were dispersed by incubation for 10 minutes with 10 uM collagenase type II (Worthington Laboratories). Cells were cultured in DMEM medium (Sigma) supplemented with 10% lipoprotein deficient serum (LPDS). Cells were identified as VSMC by their "hill and valley" growth pattern and cell populations (α-SMA+ SM-MHC+) were isolated and analyzed by fluorescence activated cell sorting (FACS)(BD ARIA).

Aortic Tissue Sectioning and Histopathological Analysis

Whole aortic arch tissue was placed in precast polyethylene molds filled with Optimal Cutting Temperature (OCT) frozen tissue matrix (Tissue-Tek). Molds were placed on dry ice and the tissue matrix was allowed to solidify completely. Sections were cut to 5-8 µm with a CM1800 cryostat microtome (Leica) set to -20°C. Sections were placed on Fisher Superfrost (Fisher Scientific) slides and allowed to dry at room temperature (RT) and stored for at -80°C in a sealed slide box. General aortic morphology was determined by hemotoxilin and eosin (H&E) staining and analyzed using an Olympus BX60 microscope.

Oil Red O Staining of Aortic Tissue Sections

For assessing neural lipid accumulation in aortic tissues, Oil Red O staining was conducted in frozen sections (8 μm) and whole *en face* longitudinal aortic arch sections. Sections were placed on slides the slides were washed with running tap water and mounted in aqueous mountant (Thermo Scientific). Images were recorded and analyzed with an Olympus BX60 fluorescence microscope connected with Cambridge Research and Instrumentation's Nuance multispectral imaging system EX. Image cubes were autoexposed and colorimetric signals were spectrally unmixed and then manually computed, comparing known signals to autofluorescence to create the spectral library. Acquired cubes were unmixed and batch processed using the spectral library to create final images. Quantification of Oil Red O staining within the sections was done with serial images and inForm software (CRi).

Determination of Global DNA Methylation in VSMCs and Aortic Tissues

DNA extracted from VSMC and aortic tissue was analyzed using 800 ng genomic DNA and Quest 5-mC DNA enzyme-linked immunosorbent assay (ELISA) Kit (Zymo Research) per manufactures' instructions

Determination of Global DNA Hydroxymethylation in VSMCs and Aortic Tissues

DNA extracted from VSMC and aortic tissue was analyzed for global DNA hydroxymethylation by T4 Phage β-glucosyltransferase treatment of DNA and analyzed using 800 ng genomic DNA and Quest 5-mC DNA ELISA Kit (Zymo Research) per manufacturer's instructions.

Locus Specific DNA Hydroxymethylation Detection in VSMC and Aortic Tissues

Sequence-specific detection of DNA hydroxymethylation was performed with the Quest 5-hmC Detection Kit (Zymo Research) per manufacturer's instructions. Genomic DNA (1 μg) was treated with T4 Phage β-glucosyltransferase. Glucosylated genomic DNA was then digested with *Msp*I, which recognizes and cleaves cytosine, methylcytosine, hydroxymethylcytosine, but not glucosyl-5-hmC hydroxymethylcytosine at CCGG loci. Locus-specific detection of 5-hydroxymethylcytosine was determined by quantitative polymerase chain reaction (qPCR) using primers designed to flank at least one *Msp*I site.

Locus Specific DNA Methylation Detection in VSMC and Aortic Tissues

Sequence-specific detection of 5- methylcytosine was performed with the Quest 5-mC Detection Kit (Zymo Research) per manufacturer's instructions. Genomic DNA (1 μg) was treated then digested with *Msp*I, which recognizes and cleaves cytosine, hydroxymethylcytosine but not 5- methylcytosine at CCGG loci. Locus-specific detection

of 5-methylcytosine was determined by qMethyl qPCR using primers designed to flank at least one *Msp*I site.

Table 1. Quantitative Polymerase Chain Reaction (qPCR) Primers

Primer	Sequence
IGF-1R Forward	5'-GTCTGGGTTCCCTTTCCAGG-3'
IGF-1R Reverse	5'-CCCTGAAGACTGCTACGCAA-3'
IGF-1R Forward	5'-TTGCCCTAAAACTGAAGCTGA-3'
IGF-1R Forward Locus 1	5'-GAGAATAGAGCCTCGCGGAC-3'
IGF-1R Reverse Locus 1	5'-GACCCCTGAAGACTGCTACG-3'
IGF-1R Forward Locus 2	5'-GCGTAGCAGTCTTCAGGGGT
IGF-1R Reverse Locus 2	5'-ACTCCGTGAAAAAGCTTCATTGTT-3'
IGF-1R Forward Locus 3	5'-AAAGCCTCGTCTTGGGGAAA-3'
IGF-1R Reverse Locus 3	5'-GCTCGGGTCCCAGTCTTAGG-3'
IGF-1R Forward Locus 4	5'-CTTCGGTGCAGGGAATGCTC-3'
IGF-1R Reverse Locus 4	5'-ACCGGAAACTTGCCTTGTTTT-3'
IGF-1R Reverse	5'-GTTCTCGCAAAGACGAAGTTG-3'
GAPDH Forward	5'-AGGTCGGTGTGAACGGATTTG-3'
GAPDH Reverse	5'-TGTAGACCATGTAGTTGAGGTCA-3'
mTOR Forward	5'-ACTGAGGAGGGAGAACAGCA-3'
mTOR Reverse	5'-CCAGTTGGTAACAATGCCATGT-3'
TET1 Forward	5'-GCAGCGTACAGGCCACCACT-3'
TET1 Reverse	5'-AGCCGGTCGGCCATTGGAAG-3'
TET2 Forward	5'-TTCGCAGAAGCAGCAGTGAAGAG-3'
TET2 Reverse	5'-AGCCAGAGACAGGGGATTCCTT-3'
TET3 Forward	5'-GACGAGAACATCGGCGGCGT-3'
TET3 Reverse	5'-GTGGCAGCGGTTGGGCTTCT-3'

Western Blot Analysis

Total proteins extracted from aortic tissue or cultured cells by RIPA buffer (Sigma) were analyzed by western blot with the following antibodies/dilutions: rabbit monoclonal anti-IGF-1R / 1:1000 (Cell Signaling) mouse monoclonal Anti-Glyceraldehyde-3-phosphate dehydrogenase (GAPDH) / 1:1000 (Sigma, USA), mouse monoclonal anti-TET1 / 1:1000 (Abcam), mouse monoclonal anti-TET2 / 1:1000 (Abcam), and mouse monoclonal anti-TET3 / 1:1000 (Abcam). Equal amounts of proteins were loaded on sodium dodecyl sulfate polyacrylamide gel electrophoresis (SDS-PAGE) gels, separated by electrophoresis and electroblotted to a polyvinylidene difluoride (PVDF) membrane. After incubation with corresponding secondary antibodies conjugated with horse radish peroxidase (HRP): Goat anti-rabbit IgG, HRP-linked antibody / 1:5000 (Sigma, USA) and Donkey anti-goat immunoglobulin G (IgG), HRP-linked antibody / 1:5000 (Sigma). Immunoreactive bands enhanced with chemiluminescence (ECL) per manufacturer's instructions (Amersham) and were visualized with a Gel Doc XR+ Imaging System (Bio-Rad).

Immunofluorescence Microscopy

Frozen sections fixed in cold acetone were blocked with 5% bovine serum albumin (BSA), 22.52 mg/ml glycine in phosphate buffered saline (PBS) + 0.1% Tween 20 (PBS-T) for 30 minutes, sections were incubated with the following primary antibodies/dilutions: rabbit monoclonal anti-IGF-1R / 1:200 (Cell Signaling), mouse monoclonal anti-TET1 /

1:200 (Abcam), mouse monoclonal anti-TET2 / 1:200 (Abcam), and mouse monoclonal anti-TET3 / 1:200 (Abcam) rabbit monoclonal anti-mTORC1 / 1:200 (Abcam) and mouse monoclonal anti-SM-actin / 1:200 (Sigma). The sections incubated with non-specific IgG set up as negative controls. Sections were washed and incubated with appropriate Alexa488 and Alexa594 1:500 conjugated secondary antibodies (Invitrogen). Sections were washed and mounted with 4',6-diamidino-2-phenylindole (DAPI)-containing Vectashield medium (Vector Laboratories). Immunofluorescent images were recorded and analyzed under Olympus FluoView FV1000 confocal microscope and Olympus BX60 fluorescence microscope connected with Cambridge Research and Instrumentation's Nuance multispectral imaging system EX. Image cubes were autoexposed and fluorescent signals were spectrally unmixed and then manually computed, comparing known signals to autofluorescence to create the spectral library. Acquired cubes were unmixed and batch processed using the spectral library to create final images.

mTOR Inhibitor Treatment

VSMCs were treated with rapamycin (25 nM), torin (15 nM) or vehicle dimethylsulfoxide (DMSO), 0.01% in DMEM 10% fetal bovine serum (FBS) for 6,12,18 or 24 h. After incubation cells were washed and total RNA was extracted for reverse transcription quantitative polymerase chain reaction (RT-qPCR).

Statistical Analysis

Data was analyzed using GraphPad Prism (GraphPad Software Inc.). Comparisons between matched pairs were performed using the Student's t-test. Multiple comparisons were performed using one-way analysis of variance (ANOVA) followed by the appropriate post-hoc test. A p-value less than 0.05 was considered significant.

Chapter 4: Results

The Development of Atherosclerosis in Diet Induced and Genetically Modified Mice

One of the leading risk factors for atherosclerotic vascular diseases is high lipid concentrations in the blood stream. In mice lacking the ApoE gene there is an increased lipid content in peripheral blood. On the other hand, these lipid levels can be modified through alterations in diet, creating susceptibility for atherosclerotic vascular diseases. To assess the development of atherosclerosis, we evaluated common areas of cardiovascular health such as weight, blood pressure, cardiac function, and aortic intimal thickness.

Assessment of Obesity in the Development of Atherosclerosis.

Various measures of obesity, including weight and BMI, have all showed a positive correlation between obesity and cardiovascular diseases, including atherosclerosis (Montenegro and Solberg 1968). To study the relationship between epigenetic alterations and atherosclerosis, a murine model of atherosclerotic plaque formation was induced via alteration of diet and/or knockout of the ApoE gene. Wild type and ApoE deficient mice fed a normal diet or chow consisting of 47% fat/kCal were studied, using animal weight as an initial indication of atherogenesis. Representative images show a visual increase in body weight and overall mass of both groups, wild type and ApoE, when subjected to a high fat diet (Figure 4). Average body weight was significantly increased between wild type mice

and wild type fed a high fat diet showing an average weight increase of 5.9 ± 1.3 grams ($P \leq 0.001$). ApoE fed a high fat diet showed a more significant average increase in weight of 8.1 ± 1.0 grams ($P < 0.0001$) vs. ApoE mice fed normal chow diet (Figure 5).

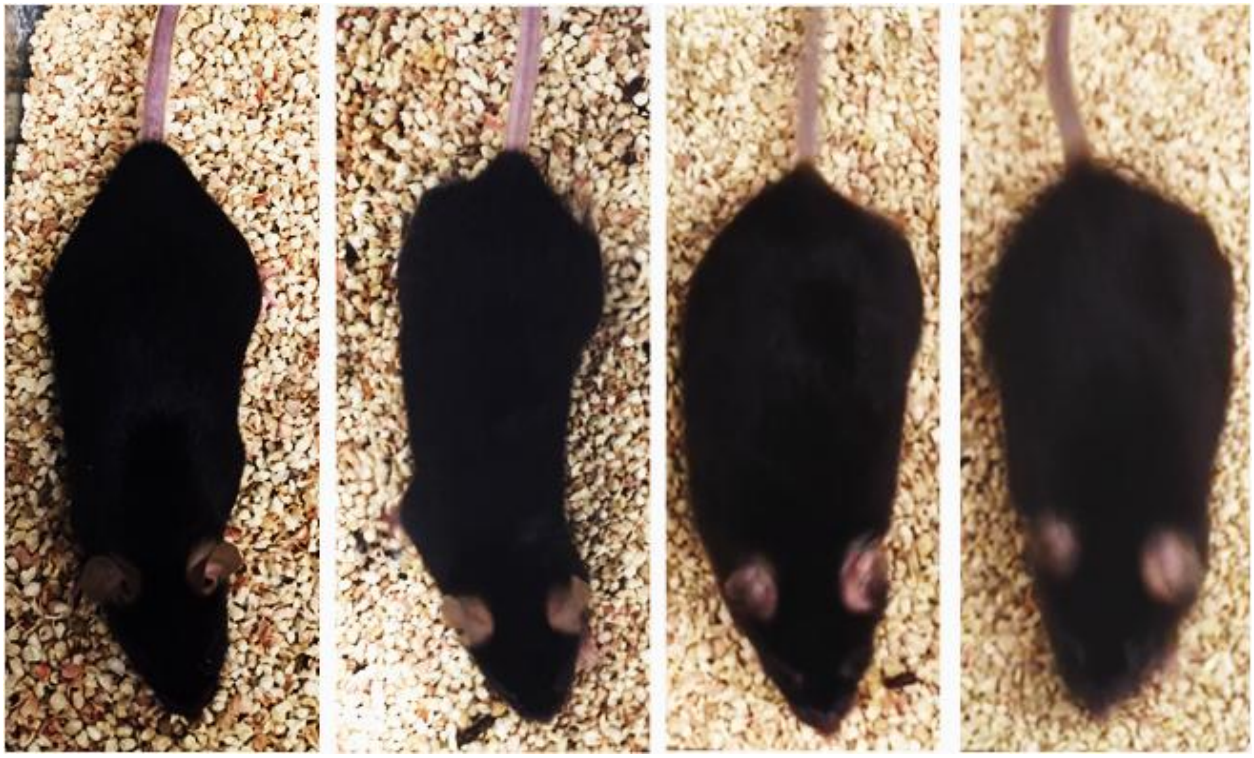

WT **APOE** **WT HF** **APOE HF**

Figure 4. Diet induced changes in wild type and ApoE knockout mice.

Representative images of wild type and ApoE mice fed normal or high fat (HF) diet demonstrating an increase in weight and BMI.

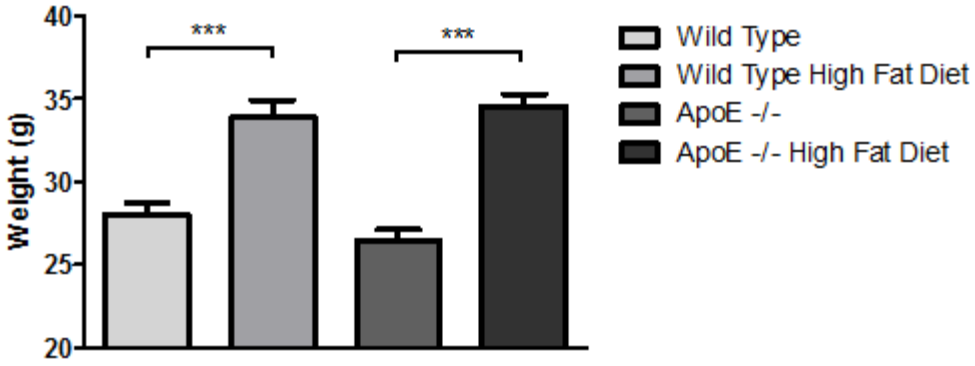

Figure 5. Average body weight in wild type and ApoE knockout mice fed normal or high fat diets.

Average body weight of wild type and ApoE deficient mice fed normal and high fat diet. Addition of a high fat diet causes a marked increase in the average body weight in both wild-type and ApoE deficient mice (n=8/group).

Consistent with weight gain through high fat diet induced obesity, wild type and ApoE deficient mice subjected to a high fat diet showed an increase in BMI. Average body mass was significantly increased between wild type mice and wild type fed a high fat diet, with an average BMI increase of 0.7 ± 0.2 kg/m^2 ($P \leq 0.0001$). ApoE mice and ApoE fed a high fat diet showed a greater average increase in BMI of 1.0 ± 0.1 kg/m^2 ($P \leq 0.0001$).

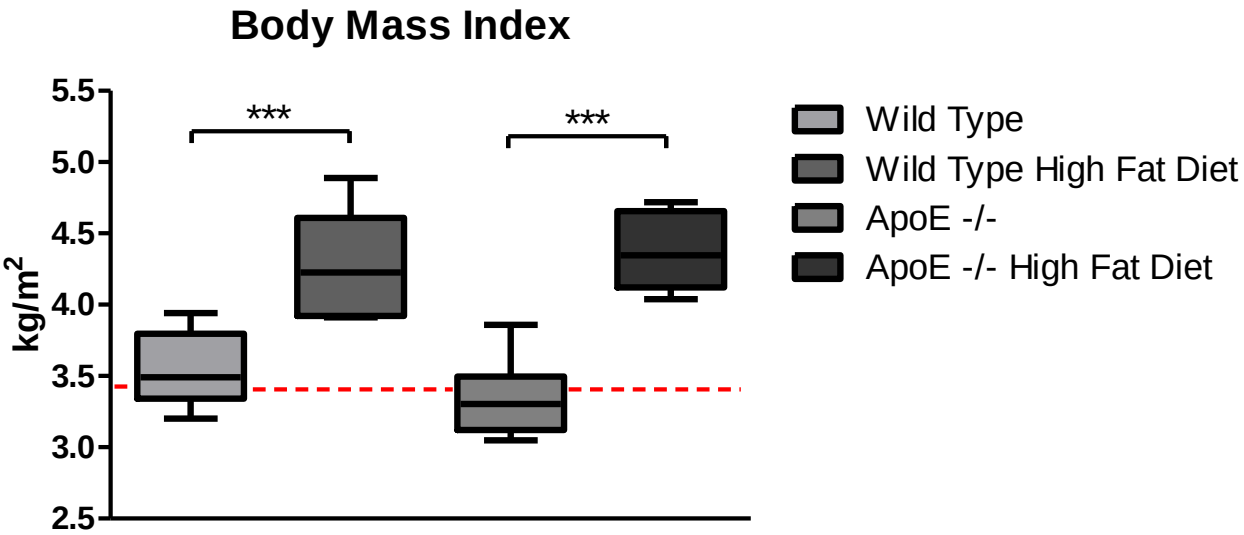

Figure 6. Body mass index changes in wild type and ApoE knockout mice fed normal and high fat diets.

Body mass index of wild type and ApoE deficient mice fed normal and high fat diets (n=8/group). BMI calculated using weight divided by average body length squared (kg/m^2). Average BMI of wild type C57Bl6J strain shown in red line from published data (Svenson KL 2015).

Assessment of Hypertension in the Development of Atherosclerosis.

Obesity resulting from high fat feeding of mice produces hyperlipidemia. Increases in lipid profiles, whether diet or genetic knockout induced, in turn, causes changes in the cellular and molecular mechanisms which have been shown to cause hypertension. Hypertension is not only a well-established cardiovascular risk factor, but also increases the risk of atherosclerosis (Alexander 1995). Thus, we next sought to assess the effect of diet and genetic knockout-induced hyperlipidemia on hypertension. Blood pressure was measured using the tail-cuff method. ApoE deficient mice showed an increase in the average systolic and diastolic pressure as compared to wild type ($P<0.005$). When subjected to high fat diet, both wild type and ApoE deficient mice showed an increase in both systolic and diastolic blood pressure over groups fed normal chow. Of the four groups, ApoE deficient fed a high fat diet showed the highest proclivity for hypertension, with five of eight mice defined as hypertensive or pre-hypertensive as characterized by a systolic pressure over 130 mmHg and a diastolic pressure over 90 mmHg.

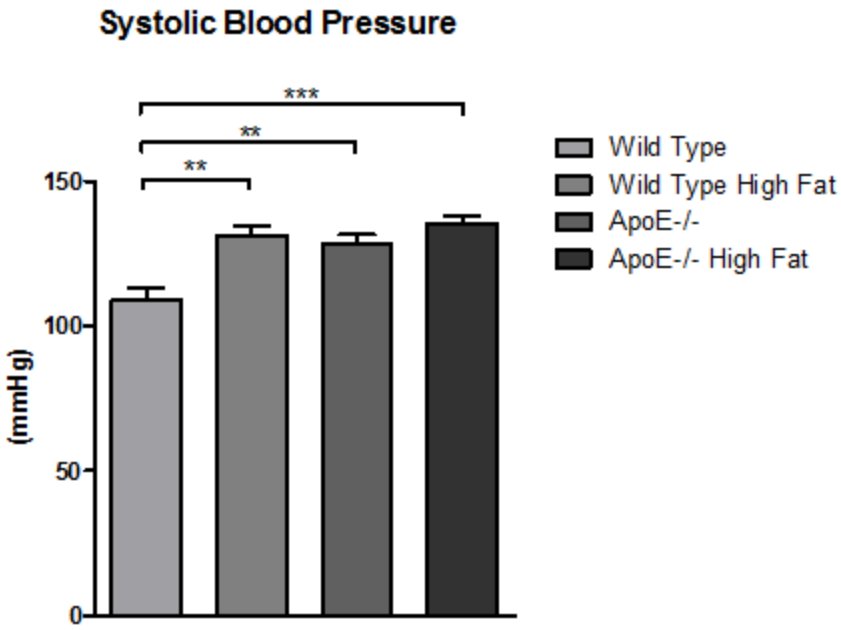

Figure 7. Systolic blood pressure of wild type and ApoE knockout mice fed normal or high fat diets.

Average systolic blood pressure by tail cuff method of wild type and ApoE deficient mice fed normal or high fat diets (n=8/group).

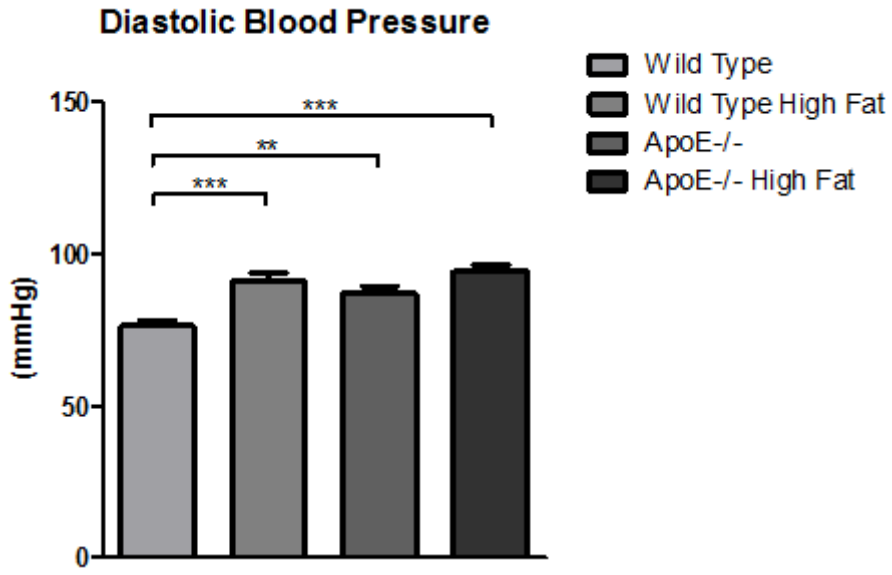

Figure 8. Diastolic blood pressure of wild type and ApoE knockout mice fed normal or high fat diets.

Average diastolic blood pressure by tail cuff method of wild type and ApoE deficient mice fed normal and high fat diets (n=8/group).

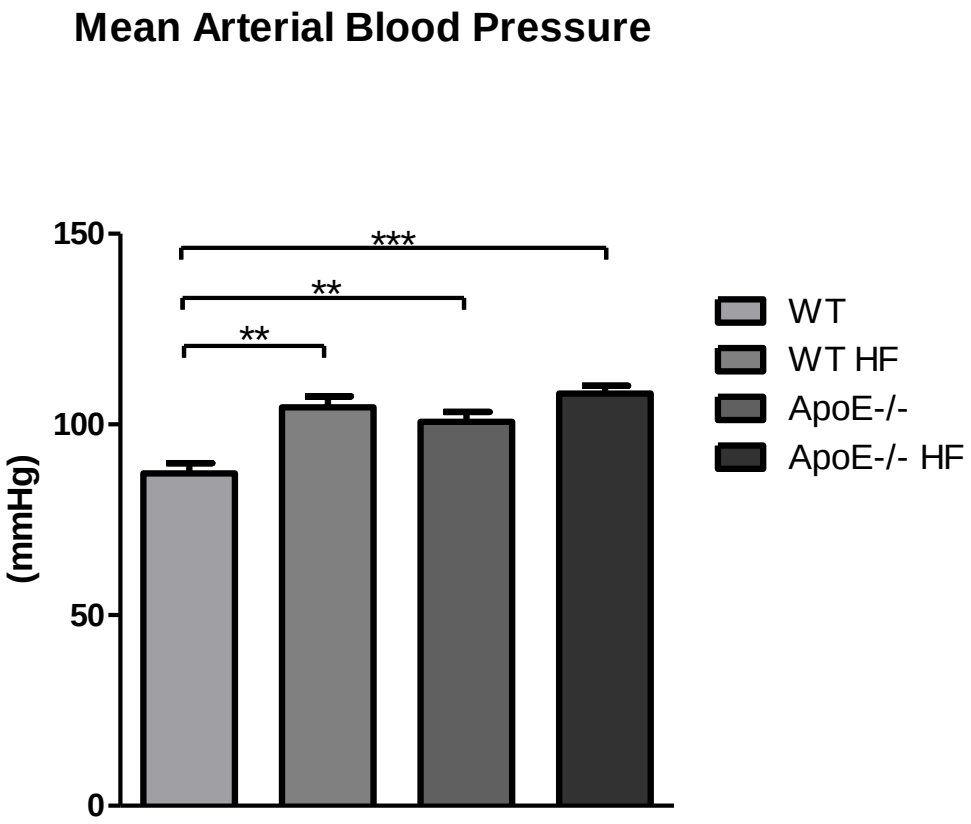

Figure 9. Mean arterial blood pressure of wild type and ApoE knockout mice fed normal or high fat diets.

Average mean arterial blood pressure derived from systolic and diastolic pressure of wild type mice and ApoE deficient mice fed normal or high fat diets. (MAP = [(2x diastolic)+systolic]/3) (n=8/group).

Assessment of Cardiac Function in the Development of Atherosclerosis.

Atherosclerosis is commonly diagnosed in a clinical setting utilizing medical and family histories, a physical exam, and various test results. Apart from diagnosis, some methods allow atherogenesis to be visualized and quantified directly though imaging modalities. One of the most commonly used modalities to assess cardiovascular function is echocardiography. Thus, we next sought to indirectly assess overall vascular health by its relation to cardiac function in diet-adjusted and/or genetic knockout-induced atherosclerosis.

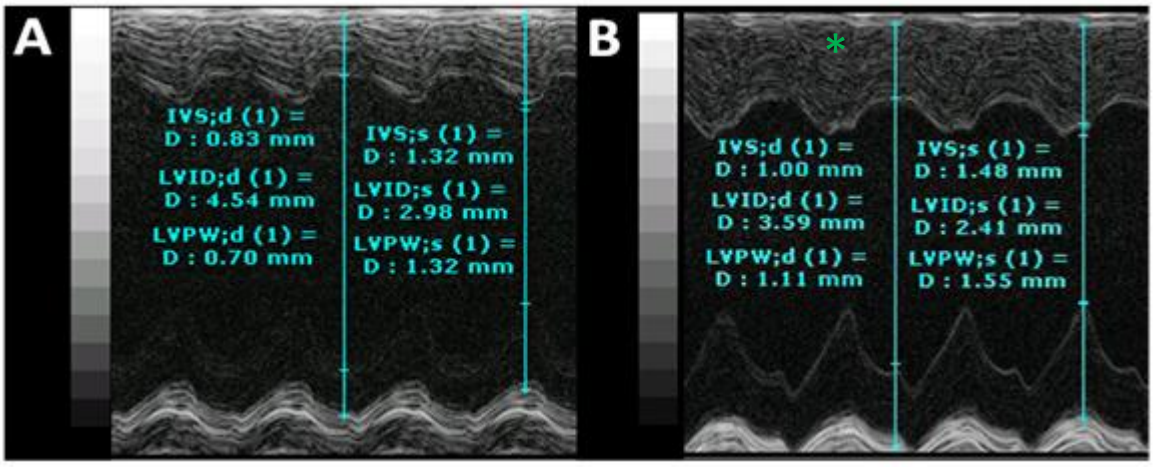

Figure 10. Echocardiography of wild type and ApoE knockout mice.

Representative echocardiographic images of left ventricles in M-mode of wild type (A) and ApoE knockout (B) showing left ventricular wall and interventricular septal thickness (denoted with green *). (LVID;s = left ventricular internal diameter systolic, LVID;d = left ventricular internal diameter diastolic, IVS;sD = interventricular septal systolic diameter, IVS;dD = interventricular septal diastolic diameter, LVPW;s = left ventricular posterior wall systolic, LVPW;d = left ventricular posterior wall diastolic)

Overall evaluation of echocardiograms of ApoE knockout mice show an increase in left ventricular wall and interventricular septal thickness as compared to wild type mice (Figure 10). Furthermore, transthoracic echocardiographic measurements showed a significant decrease in fractional shortening, left ventricular internal diameter during systole (LVID;s), left ventricular internal diameter during diastole (LVID;d) and an increase in the interventricular septal diameter (IVS) that was exacerbated by the addition of high fat diet feeding and the genetic knockout of ApoE ($P < 0.05$) (Table 2).

Table 2. Echocardiographic measurement of heart function and wall motion in wild type and ApoE mice fed normal or high fat diets.

Animal Group	**Wild Type**	**Wild Type High Fat**	**ApoE$^{-/-}$**	**ApoE$^{-/-}$ High Fat**
Heart Rate (beats/min)	399±19	416±21	394±15	395±17
Fractional Shortening (%)	37.7±1.2	32.5±1.5*	32.1±1.9*	29.5±2.1*†
LVID;s (mm)	2.89±0.09	2.81±0.11	2.48±0.07*†	2.46±0.06*†
LVID;d (mm)	4.64±0.08	4.16±0.13*	3.65±0.09*†	3.49±0.11*†‡
IVS (mm)	1.09±0.05	1.21±0.1*	1.24±0.09*†	1.31±0.07*†‡

Transthoracic echocardiographic measurements in M-Mode of mice. Values represented as

Mean ± SEM (n=8/group).

*Significant difference vs Wild Type mice.
†Significant difference vs Wild Type High Fat mice ApoE-/- mice.
‡Significant difference vs ApoE-/- mice.

Transthoracic Aortic Ultrasound Assessment in the Development of Atherosclerosis.

There is close association between cardiac hypertrophy and dysfunction and vascular health due to the causative nature of vascular thickening, occlusion, and stenosis associated with atherosclerosis. Thus, to assess vascular health and function during the progression of atherosclerosis, we next sought to evaluate aortic arch intimal thickness via transthoracic aortic ultrasound (Figure 11).

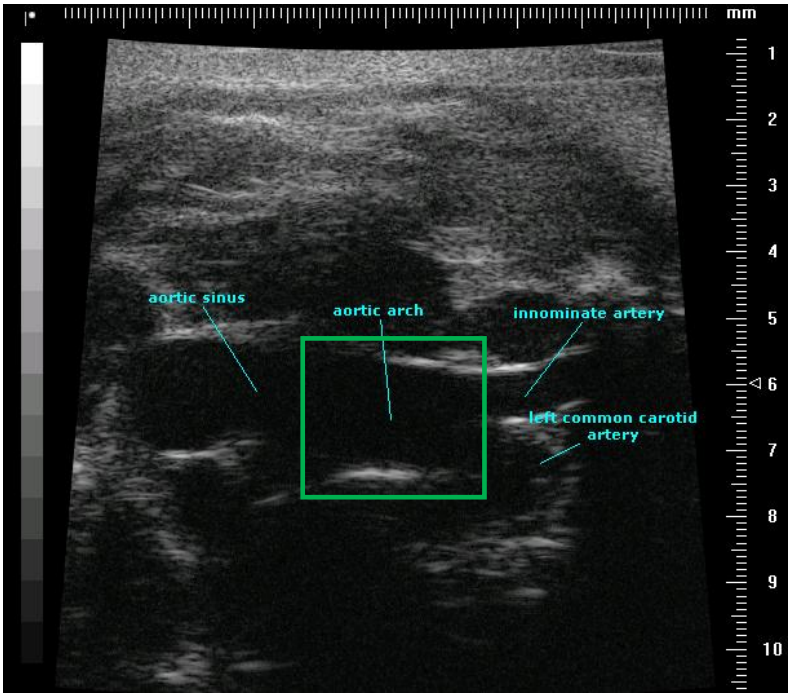

Figure 11. Ultrasound examination of arterial gross anatomy in wild type mice. Representative transthoracic echocardiography showing the location of aortic arch (denoted with green box). Measurements taken in B-mode during systole.

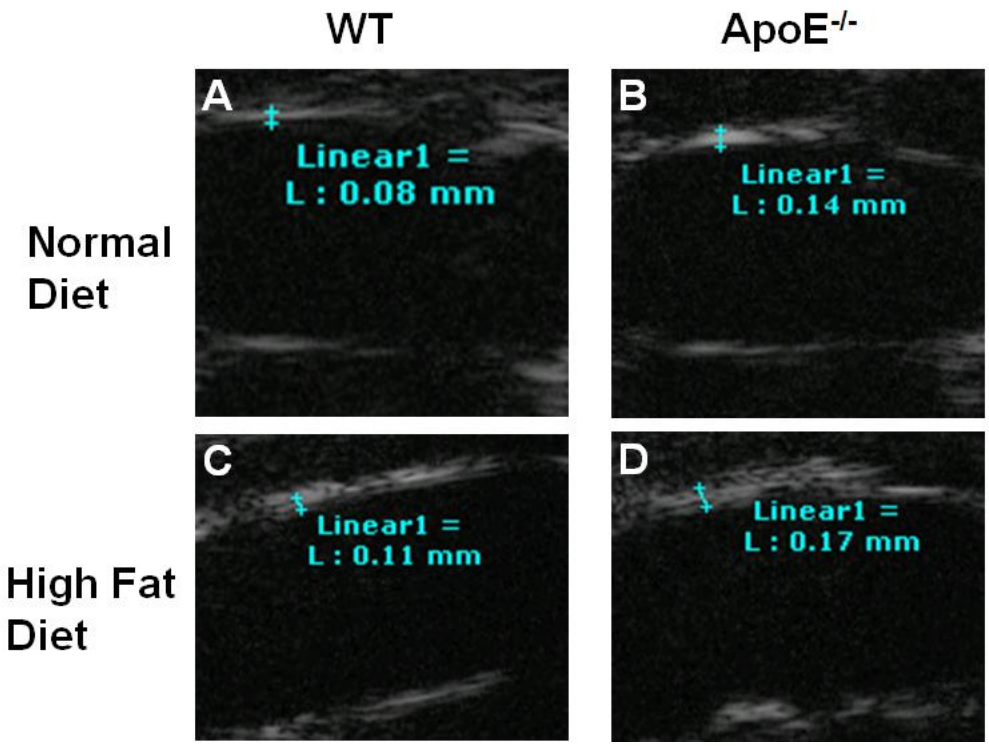

Figure 12. Ultrasound examination of aortic intimal thickness.

Representative transthoracic echocardiographic measurements of aortic arch intimal thickness in B-mode of wild type and ApoE knockout fed normal chow, (A) and (B) respectively, and wild type and ApoE knockout fed a high fat diet, (C) and (D) respectively.

Significantly increased average intimal thickness was observed within the aortic arch of wild type mice subjected to a high fat diet as compared to wild type control (P=0.03). Similarly, an increase in intimal thickness was observed between wild type and ApoE knockout mice fed a normal diet (P=0.004), with the most dramatic increase seen in ApoE knockout mice fed a high fat diet, as compared to wild type control mice (P=0.001) (Figure 13).

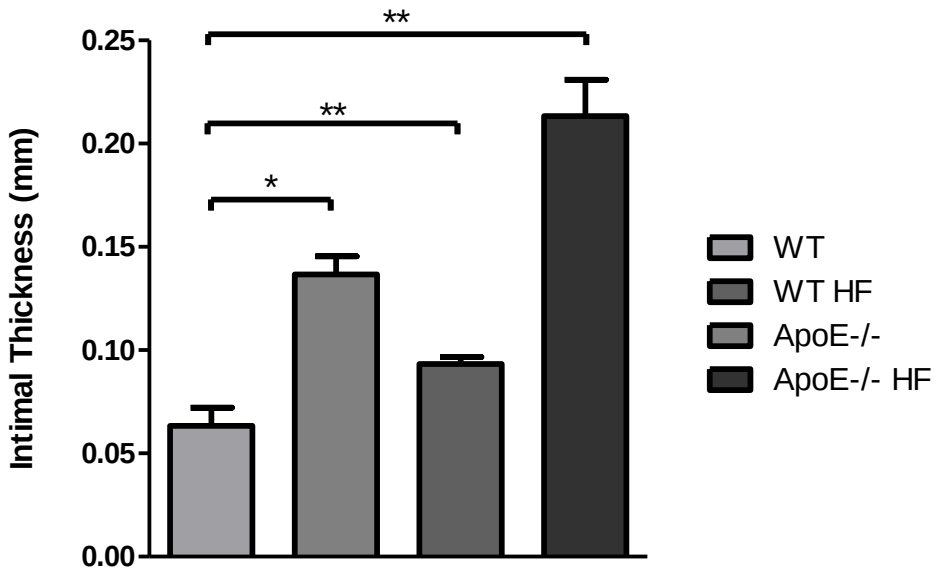

Figure 13. Average aortic intimal thickness by ultrasound examination.

Average transthoracic aortic intimal thickness measurements by ultrasound examination in B-mode of wild type and ApoE knockout mice fed normal or high fat diets (n= 3/group).

Ex Vivo Assessment of Lipid Inclusion in Atherosclerosis

Extracellular lipid accumulation and intracellular lipid inclusion via endocytosis is a central mechanistic process in the development of atherosclerotic progression. To visualize the inclusion of neutral lipids within the atherosclerotic plaque, whole longitudinal aortic arch sections were taken from wild type and ApoE mice fed either a normal or high fat diet and stained with Oil Red O. Marked increases in number and severity of plaques were seen in ApoE mice as compared with wild type. Additionally, Oil Red O staining was increased in both groups with the addition of a high fat diet (Figure 14).

Next, transverse aortic arch sections were stained with Oil Red O. As expected, atherosclerosis prone ApoE deficient mice fed normal chow developed fibrous plaques in the aortic wall. Conversely, no atherosclerotic lesions existed in sex- and age-matched wild type mice, and only intermittent small areas showed any lipid inclusion (Figure 15).

Finally, serial transverse aortic arch sections were stained with Oil Red O and showed significant increases in the quantification of staining in ApoE mice as compared with wild type, which was further increased with the addition of a high fat diet ($P<0.05$) (Table 3).

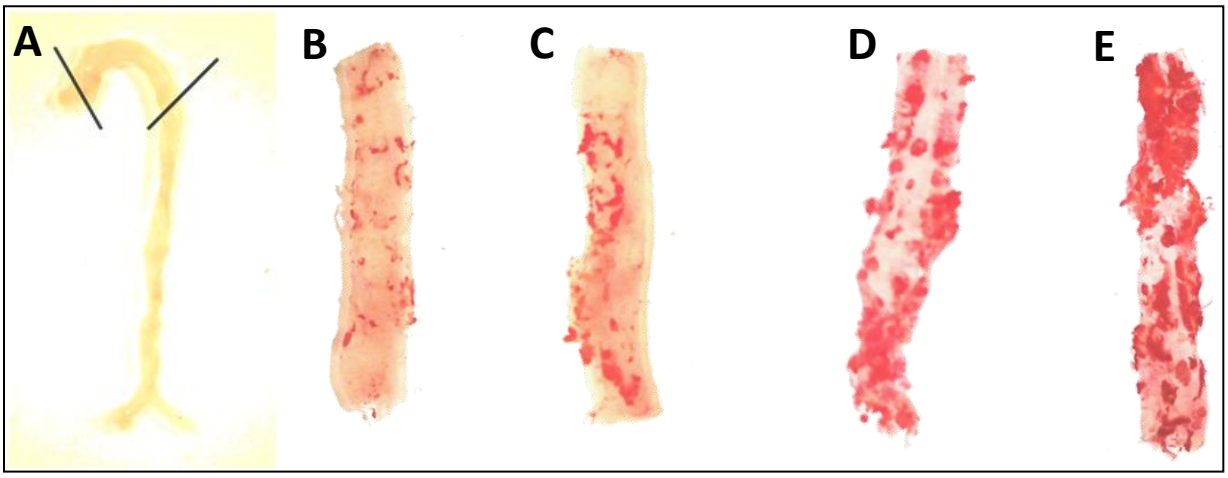

Figure 14 *En face* Oil Red O staining of whole aortic arch segments of WT and ApoE mice fed normal or high fat diets.

(A) Representative area of whole aortic arch segment taken for analysis of lipid inclusion and plaque formation. Oil Red O staining of whole aortic arch segments in (B)wild type normal diet, (C) wild type fed a high fat diet (D) ApoE normal diet, and (E) ApoE fed a high fat diet.

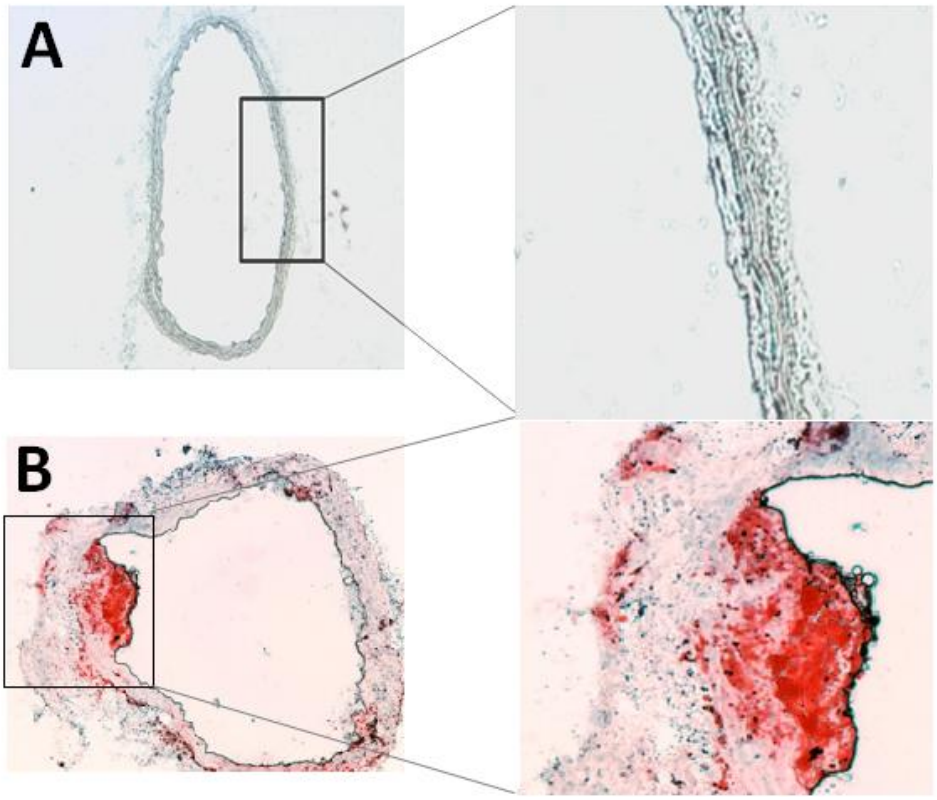

Figure 15. Oil Red O staining of aortic wall sections from wild type and ApoE knockout mice.

Representative aortic arch cross section of wild type (A) and ApoE (B) stained for Oil Red O.

Table 3. Quantification of atherosclerotic plaques stained with Oil Red O.

	Wild Type	**ApoE$^{-/-}$**
Normal Diet	1.1±0.3	25.3±3.2 *
High Fat Diet	16.7±5.3 *†	31.9±7.8 *†‡

Quantification of Oil Red O staining within the aortic arch with serial cross section images obtained using Nuance TRIO(CRi) multispectral analysis and inForm software. Data is expressed as Means ± SEM, statistical analysis via One-way ANOVA (n=8/group)

*Significant difference vs Wild Type mice.

†Significant difference vs Wild Type High Fat mice ApoE-/- mice.

‡Significant difference vs ApoE-/- mice.

Global DNA methylation and hydroxymethylation in the aortas of wild type and ApoE knockout mice fed normal or high fat diets.

Aberrant DNA methylation is related not only to aging, but also the onset and progression of numerous diseases, and, because of its affect on numerous gene promoters, aberrant methylation patterns may be an important contributor to the progression of atherosclerosis (Dong, Yoon et al. 2002). To test whether DNA methylation differed during the progression of atherosclerosis global 5-methylcytosine levels were analyzed. A positive correlation was observed between global demethylation and knockout of ApoE, as well as, the addition of a high fat diet ($P<0.05$) (Figure 16). The greatest progression of atherosclerosis, as evidenced by physiological and *ex vivo* examination, was seen in the ApoE genetic knockout group fed a high fat diet which showed the greatest average demethylation as compared to the wild type group fed normal chow ($P<0.001$).

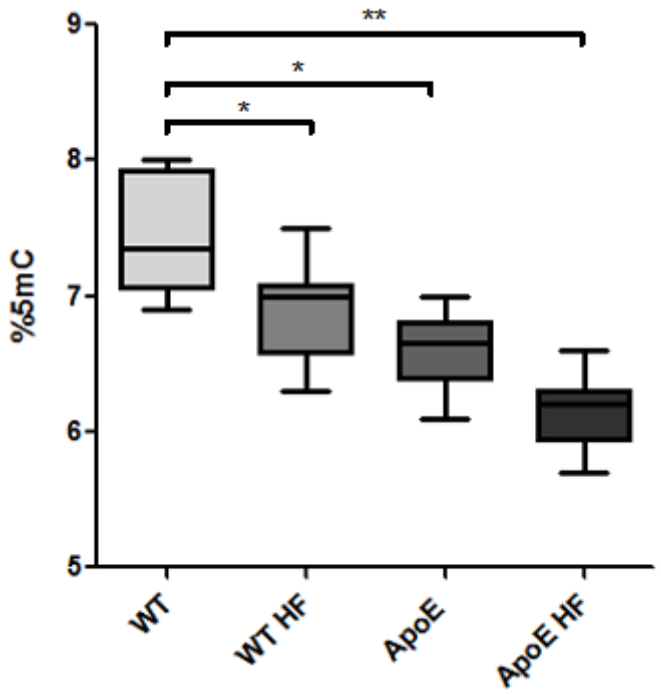

Figure 16. Assessment of Global DNA methylation levels in wild type and ApoE knockout mice fed normal or high fat diets.

Quantification of global 5-methylcytosine concentration within aortic arch of wild type and ApoE deficient mice fed normal or high fat diet. Analysis via 5-mC ELISA (n=8/group).

Because aberrant DNA methylation patterns are common to diseased states, and because aberrant 5-methylcytosine levels were observed during the progression of atherosclerosis, we next analyzed global 5-hydroxymethylcytosine levels. Fluorescence microscopy of whole aortic sections provides unclear expression levels (Figure 17), however, similar to 5-methylcytosine levels, there was a positive correlation between global loss of hydroxymethylation and the level of atherosclerosis as assessed by DNA ELISA. The ApoE genetic knockout group fed a high fat diet showed the largest global loss of 5-hydroxymethycytosine as compared to the control wild type group fed normal chow ($P<0.01$) (Figure 18).

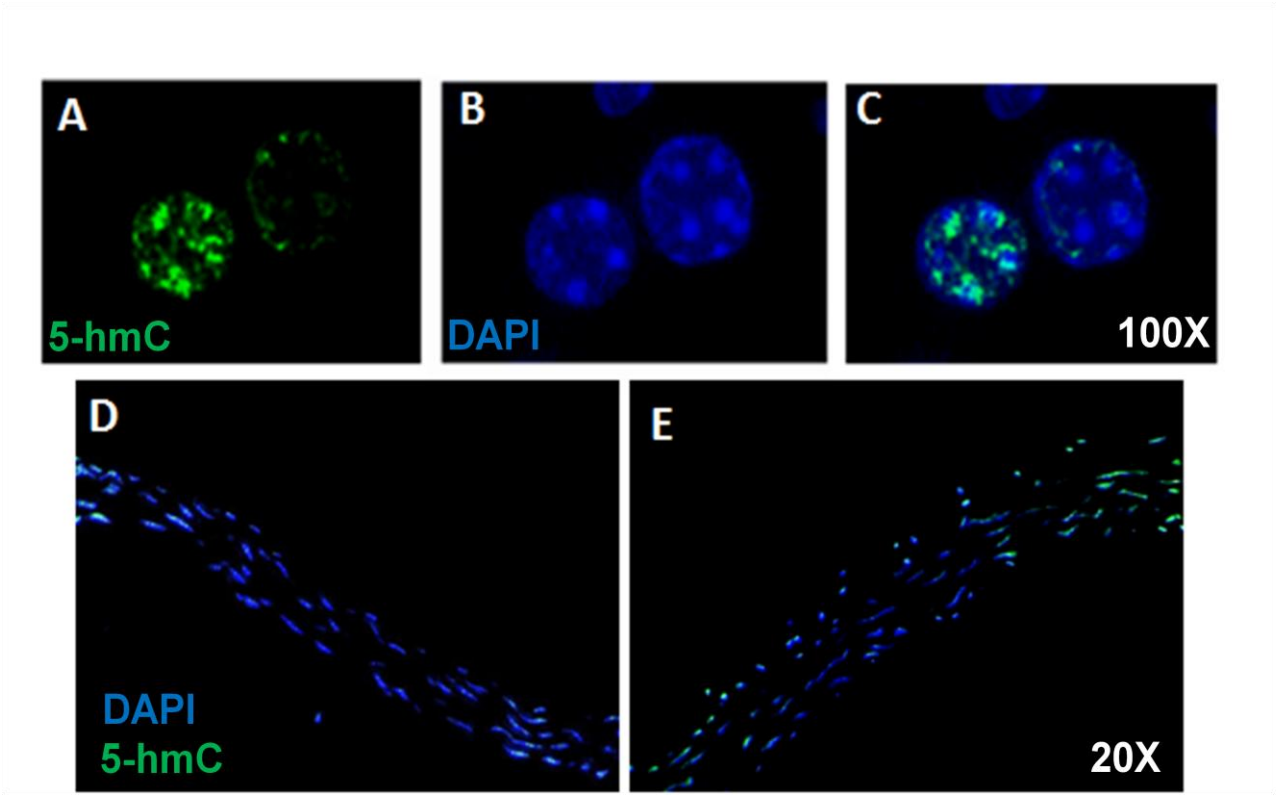

Figure 17. *In situ* fluorescence microscopy of DNA hydroxymethylation

Fluorescence microscopy of anti-5-hydroxymethylcytosine (A), DAPI (B) and merged (C) showing nuclear localization in aortic VSMC. Wild type (D) and ApoE knockout (E) aortic arch cross section showing distribution of anti-5-hydroxymethylcytosine.

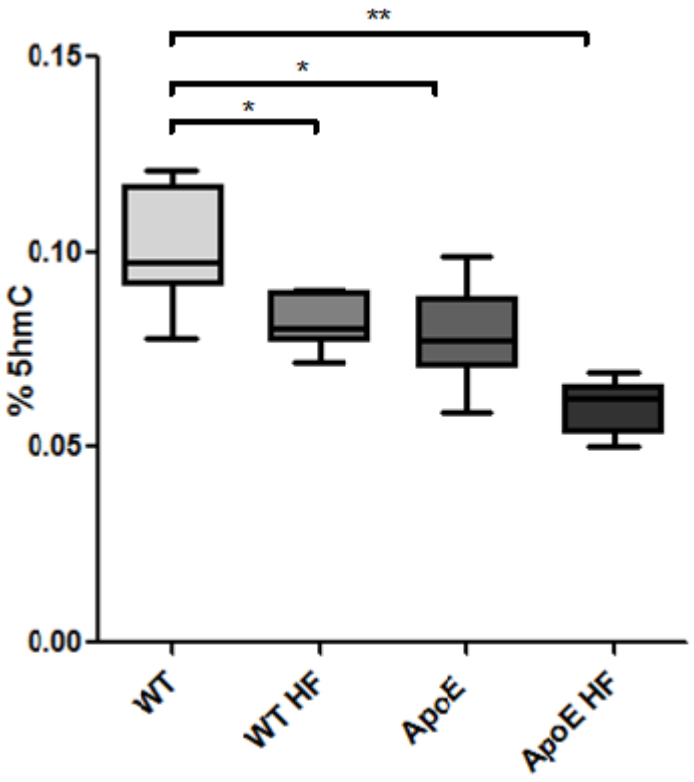

Figure 18. Assessment of global DNA hydroxymethylation levels in the aortas of wild type and ApoE mice fed normal or high fat diets.

Assessment of global DNA 5-hydroxymethylcytosine levels in the aortic arch of wild type and ApoE knockout mice fed normal or high fat diet. Analysis via 5-hmC ELISA (n=8/group).

Locus Specific Epigenetic DNA Alterations

The correlation between genome-wide aberrant expression levels of methylation and hydroxymethylation and progression of atherosclerosis may suggest that these mechanisms play a role in the development of the disease. To determine the effects of methylation and hydroxymethylation in the pathogenesis of atherosclerosis, locus specific levels of 5-methylcytosine and 5-hydroxymethylcytosine within the promoter and proximal enhancer region were tested for in a selection of genes relating to atherosclerosis. A selection of genes were tested based on three criteria: 1) An association or link with cardiovascular disease through associated studies 2) The presence of CpG island within the promoter or proximal enhancer region 3) The ability to make primers for glycosylation-coupled qPCR and that can be enzymatically cleaved by MspI. Within the selection of genes, only a few genes showed a significant difference in the level of hydroxymethylation between wild type and ApoE groups.

Assessment of IGF-1R Expression in Aortas of Wild Type and ApoE Mice

Because DNA methylation and hydroxymethylation are major epigenetic modifications of the genome, they have the potential to silence and induce gene expression. Additionally, because of a relatively low level of 5-hydroxymethylcytosine within the genome, changes often result in significant epigenetic control, which result in changes in protein expression (Wossidlo, Nakamura et al. 2011). Of the genes tested for the presence of 5-hydroxymethylcytosine, IGF-1R had significant differences in ApoE as compared to wild type control mice (P-value ≥ 0.05). Because of these differences in the presence of

5-hydroxymethylcytosine, IGF-1R expression was further analyzed both at the level of transcription and at the level of protein expression. The expression of IGF-1R in wild type and ApoE deficient mice was examined in serial aortic sections by fluorescence microscopy and a notable lack of IGF-1R and α-SM-actin immunostains (star) and certain areas of stains for IGF-1R (arrow) were observed in the ApoE knockout aortic plaque (Figure 19).

IGF-1R expression was further analyzed during a range of 9 months from 3 month to one year old wild type and ApoE deficient mice (Figure 20). A significant decrease in IGF-1R expression was seen in ApoE in all age ranges as compared to wild type ($P<0.05$), and ApoE deficient mice showed a decrease that positively correlated with aging.

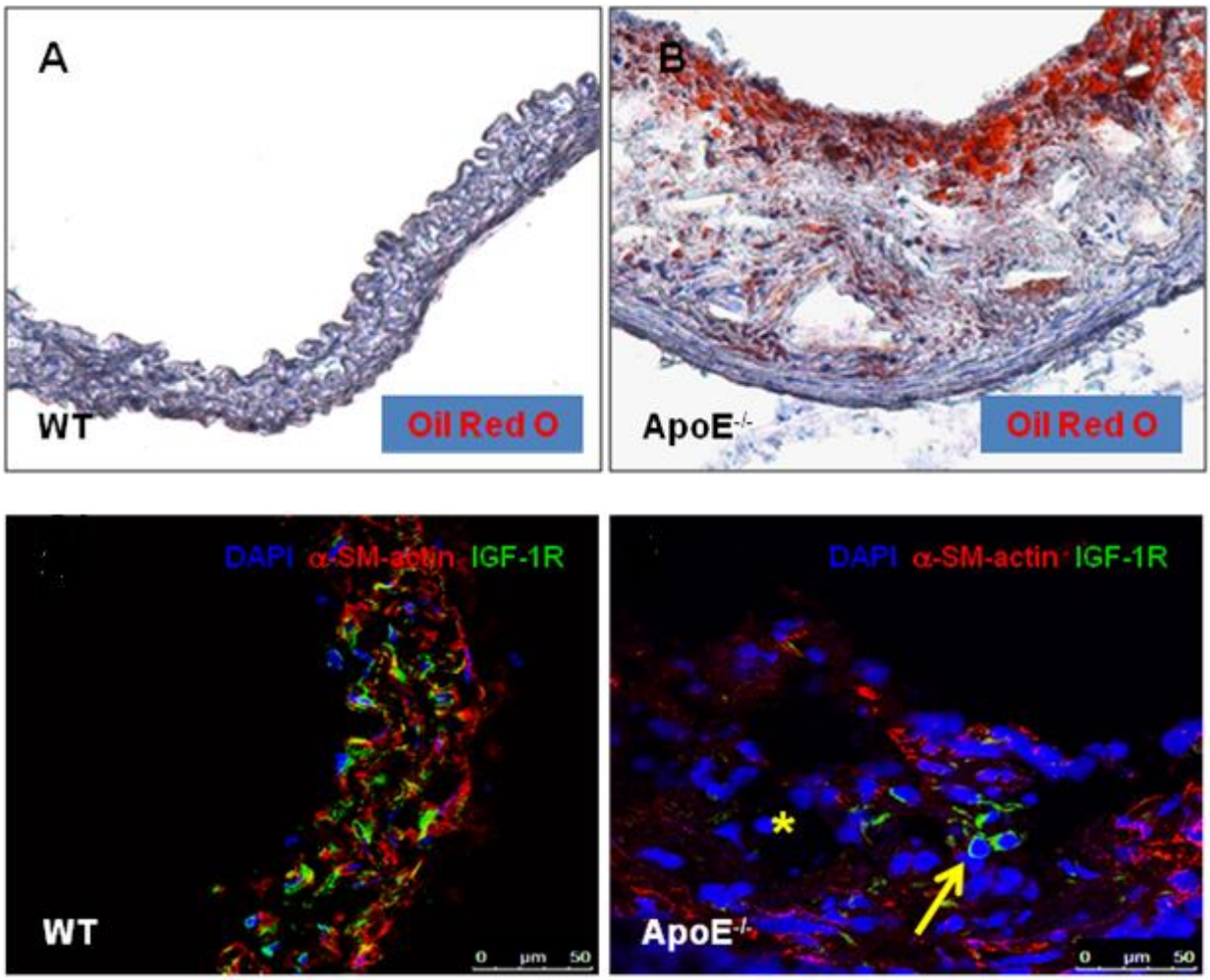

Figure 19. Immunofluorescence microscopy of IGF-1R in wild type and ApoE knockout aortas.

WT and ApoE knockout aortas immunostained with antibodies against IGF-1R (green) and α-SM-actin (red). Nuclear counter-staining (blue) was conducted with DAPI in the same sections. Note a lack of IGF-1R and α-SM-actin immunostains (star) and certain areas of stains for IGF-1R (arrow) in the ApoE knockout aortic plaque.

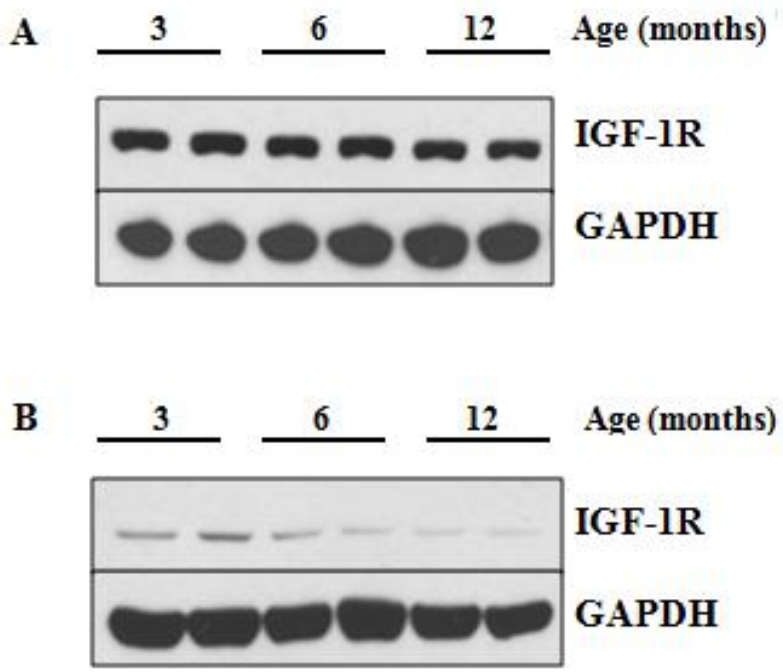

Figure 20. Expression of IGF-1R protein in wild type and ApoE knockout mice during aging.

Protein expression levels of IGF-1R in (A) wild type and (B) ApoE knockout mice during aging. Expression levels assessed by western blot analysis from protein extracted from aortic VSMCs from 3, 6, and 12 month old mice. (n=2/group)

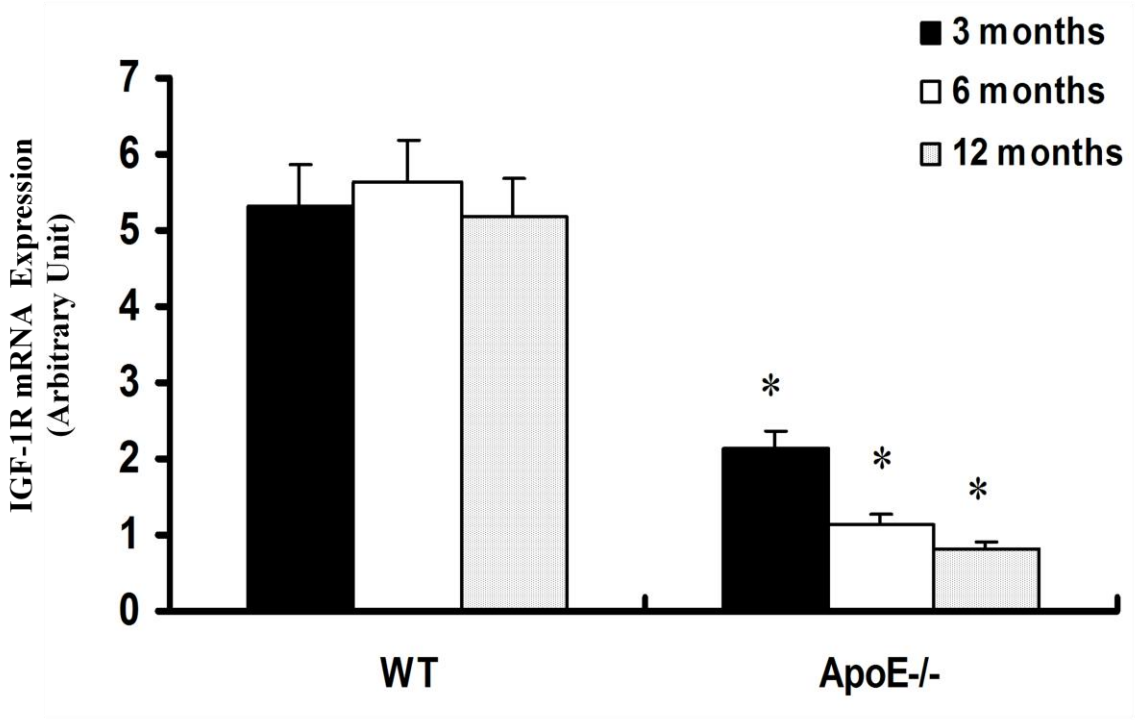

Figure 21. Expression of IGF-1R mRNA in wild type and ApoE during aging.

mRNA expression levels of IGF-1R in wild type and ApoE knockout mice during aging. Expression levels assessed by RT-qPCR analysis from RNA extracted from aortic VSMCs from 3, 6, and 12 month old mice. (n=3/group)

Assessment of 5-Methylcytosine and 5-Hydroxymethylcytosine Levels in IGF-1R Gene Promoter and Surrounding Regions.

Of the genes tested for the presence of 5-hydroxymethylcytosine, IGF-1R had a significant differences (P-value ≥ 0.05). To further analyze the epigenetic changes four loci were selected within the proximal enhancer and promoter region and analyzed for the presence of 5-methylcytosine and 5-hydroxymethylcytosine (Figure 22).

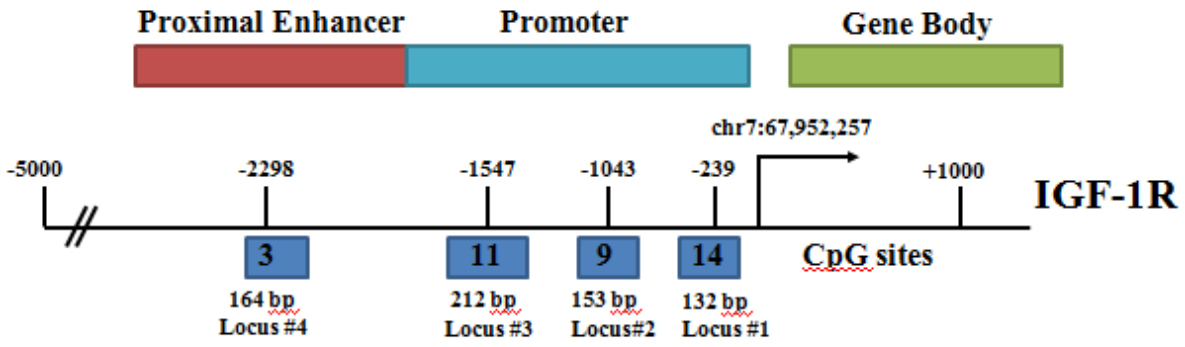

Figure 22. Schematic representation of IGF-1R gene promoter and surrounding regions.

Genetic map of IGF-1R showing four loci tested for of 5-methylcytosine and 5-hydroxymethylcytosine by qMethyl and glycosylation-coupled qPCR. Locations shown from transcription start site (TSS) in base pairs above line. Size of qPCR amplicon and number of CpG sites shown below line and in blue boxes.

To verify successful amplification, genomic DNA from wild type mice was treated with hydroxymethylcytosine glucosyltransferase and subsequently amplified via PCR. All loci treated showed successful amplification by qPCR (Figure 23).

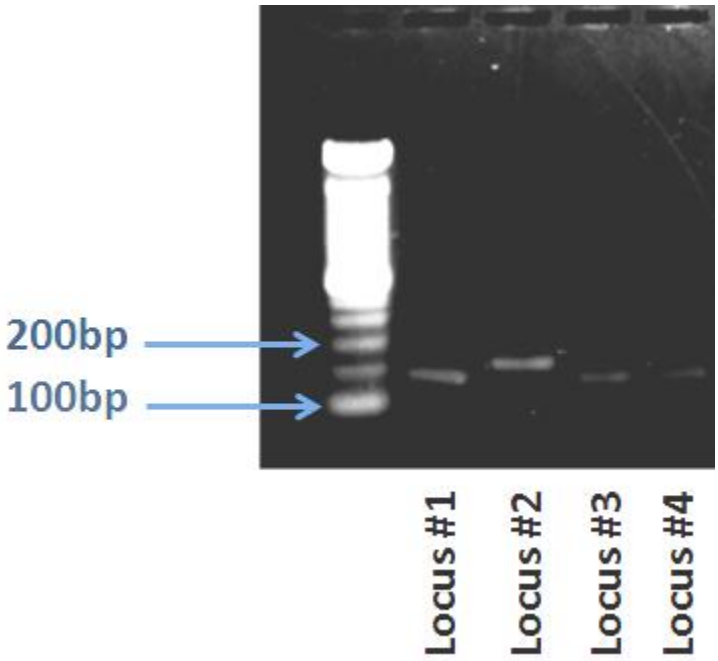

Figure 23. Verification of Glucosylation-Coupled qPCR Products for IGF-1R Loci.

Verification of glucosylation-coupled qPCR products for IGF-1R loci using wildtype genomic DNA treated with hydroxymethylcytosine glucosyltransferase but not digested with MspI.

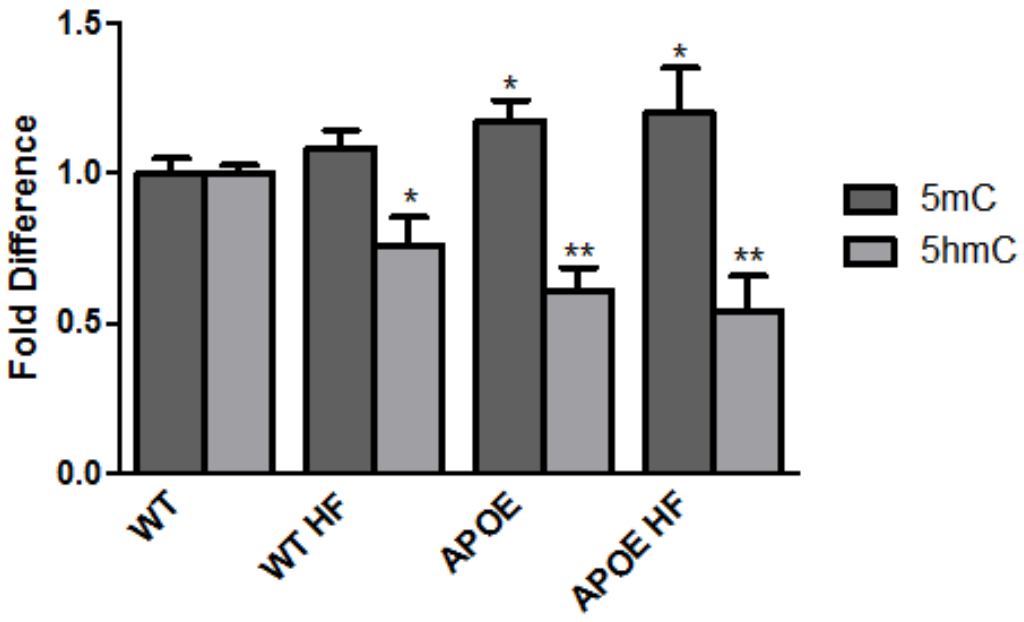

Figure 24. DNA methylation and hydroxymethylation in IGF-1R promoter region.

Comparison of average DNA methylation and hydroxymethylation within the promoter and proximal enhancer region of IGF-1R in wild type and ApoE knockout mice fed normal or high fat diets.

All four loci were tested first for differences in 5-hydroxymethylcytosine and 5-methylcytosine levels (Figure24) . ApoE knockout mice showed a decrease in the amount of hydroxymethylation as compared to wild type controls ($P<0.01$). Addition of a high fat diet alone and in combination with the genetic knockout of the ApoE gene caused progressive reductions in the amounts of 5-hydroxymethylcytosine as compared to wild-type control across all four loci tested ($P<0.05$) (Figure 24). Conversely, ApoE mice showed an increase in the amount of methylation as compared to wild type controls across all four loci. Additionally, ApoE genetic knockout mice with and without the introduction of a high fat diet caused increases in the average amount of 5-methylcytosine as compared to wild type control ($P<0.05$).

TET Methylcytosine Dioxygenase Enzymes in Atherosclerosis

The conversion of the base 5-methylcytosine to 5-hydroxymethylcytosine is governed by the Ten-eleven translocation (TET) methylcytosine dioxygenase family of enzymes. To determine which member of the TET family may be involved in this conversion, mRNA expression of all TET enzymes were analyzed by RT-qPCR in wild type mice. Of the enzymes tested TET2 had the highest and only significant level of expression ($P<0.001$) (Figure 25).

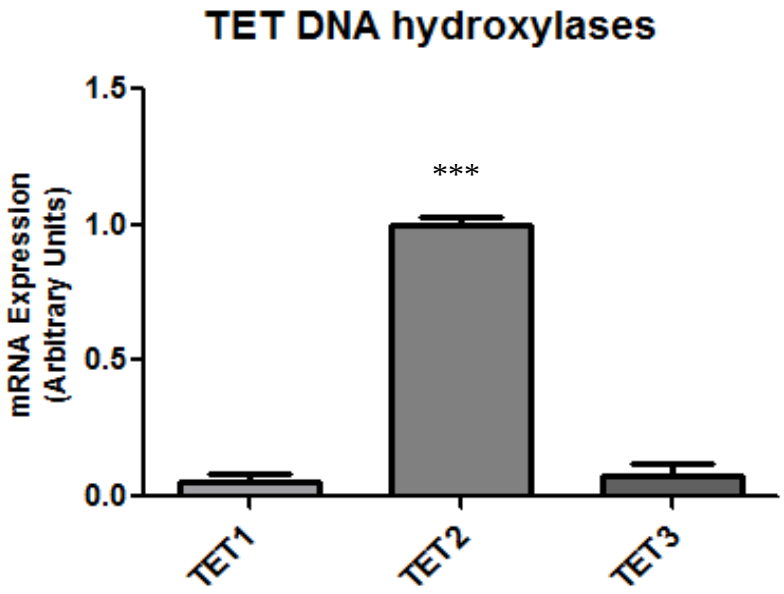

Figure 25. Assessment of TET mRNA expression in wild type mice.

Assessment of.of TET1,2, and 3 mRNA transcript levels in vascular aortic arch cells of wild type mice by RT-qPCR. (n=3/group)

TET2, shown to have the highest level of expression, was then analyzed by RT-qPCR in wild type and ApoE knockout mice. A significant decrease in the amount of TET2 was observed both in mRNA and protein expression levels by immunoflurescent microscopy (Figure 26, 27). Expression of TET2 mRNA was further shown to be down-regulated by the addition of a high fat diet, with ApoE knockout mice fed a high fat diet displaying the lowest expression ($P<0.01$) (Figure 27).

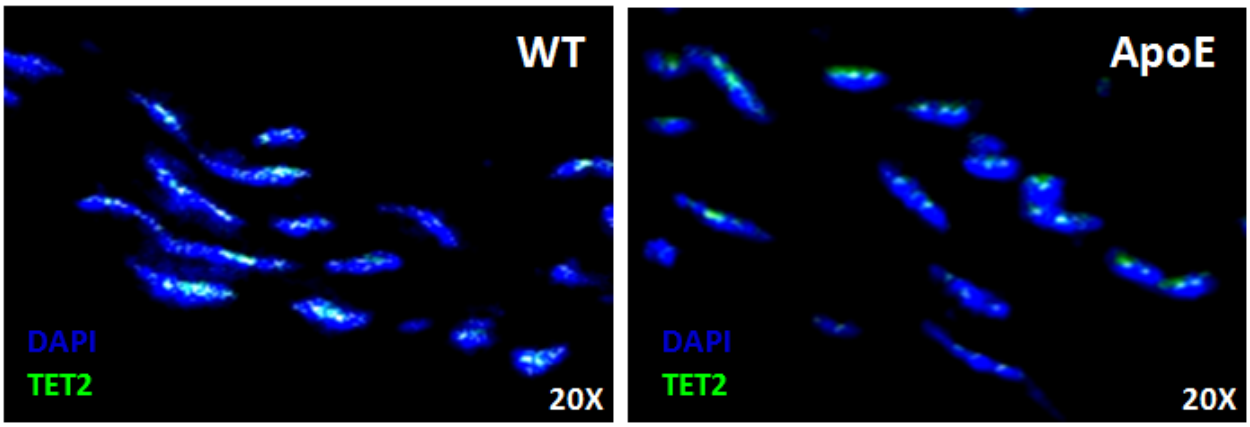

Figure 26. Immunofluresecence microscopy of TET2 expression in wild type and ApoE aortas.

WT and ApoE knockout aortas immunostained with antibody against 5-hydroxymethylcytosine (green) and nuclear counter-stained with DAPI (blue). Note a lack of expression of TET2 in the ApoE knockout aorta.

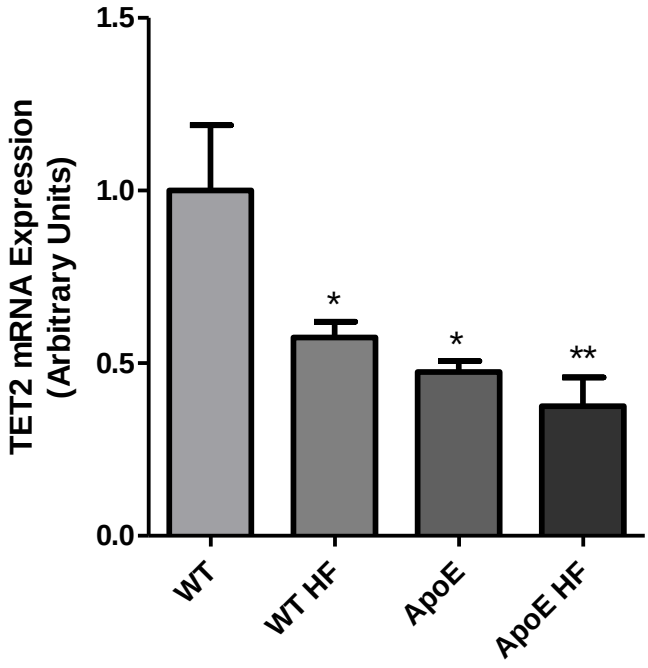

Figure 27. Assessment of TET2 mRNA expression in wild type and ApoE fed normal or high fat diets.

Expression of TET 2 mRNA transcript levels by RT-qPCR in vascular aortic arch cells of wild type and ApoE knockout mice fed normal or high fat diets. (n=3/group)

mTOR Expression in Atherosclerosis

Mechanistic target of rapamycin (mTOR) is a master regulator of cell growth, proliferation, motility, survival, protein synthesis, autophagy, and transcription. The complex mTORC1 acts as a nutrient/energy/redox sensor and controls protein synthesis, becoming active in the presence of increased cellular nutrient, oxygen, and energy levels (Weichhart 2012). We therefore assessed the expression of mTORC1 in wild type vascular smooth muscle cells (VSMC), as well as cells deficient in the ApoE protein. mTORC1 expression was higher in VSMCs deficient in ApoE and showed increases in cellular localization via immunoflurescent microscopy (Figure 28).

To determine the affect of diet on mTOR, mRNA transcript levels were analyzed in wild type and ApoE deficient mice with and without the addition of a high fat diet. As expected, both wild type and ApoE mice fed the high fat diet showed significant increases in the expression levels of mTOR. Wild type fed the high fat diet showed an approximately four fold increase in mTOR levels (Figure 29).

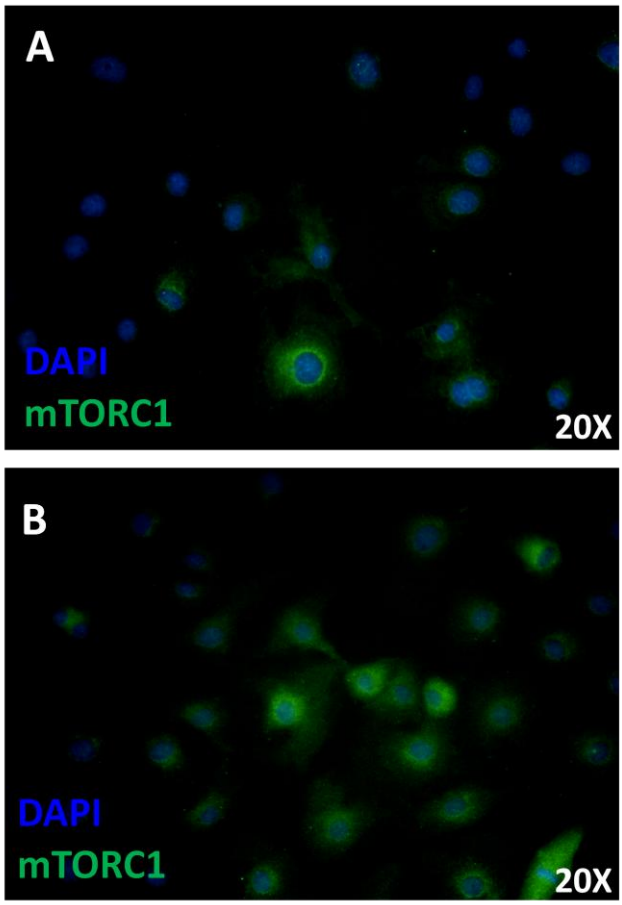

Figure 28. Immunofluresecence microscopy of mTORC1 in wild type and ApoE VSMCs.

Wild type (A) and ApoE knockout (B) aortic VSMCs grown in chamber-slides were fixed and immunostained with monoclonal antibody against mTORC1 (green) and nuclear counter-stained with DAPI (blue). Note increased expression of mTORC1 in the ApoE knockout VSMCs.

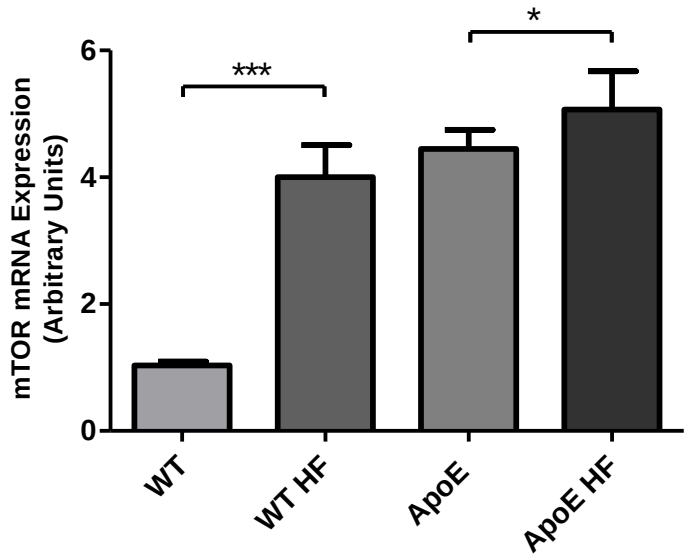

Figure 29. Assessment of mTOR mRNA expression in wild type and ApoE mice fed normal or high fat diets.

Expression of mTOR mRNA transcript levels by RT-qPCR in vascular aortic arch cells of wild type and ApoE knockout mice fed normal or high fat diets. (n=8/group)

Rapamycin and torin are inhibitors of the mTOR pathway. Because our data suggested that the induction of the major nutrient sensing and growth pathway, mTOR, through diet and genetic knockout of ApoE correlated with reductions in TET2 expression we sought to define the effects of inhibition of mTOR on TET2.

Rapamycin inhibits mTOR by binding to its FKBP12 receptor, the FKBP12 complex then binds directly to the FKBP12-Rapamycin Binding (FRB) domain of mTOR, thereby inhibiting its activity (Marx, Jayaraman et al. 1995). As expected, treatment of wild type VSMCs with either rapamycin or torin produced a significant decrease in mTOR mRNA transcript expression in a time dependent manor (Figure 30).

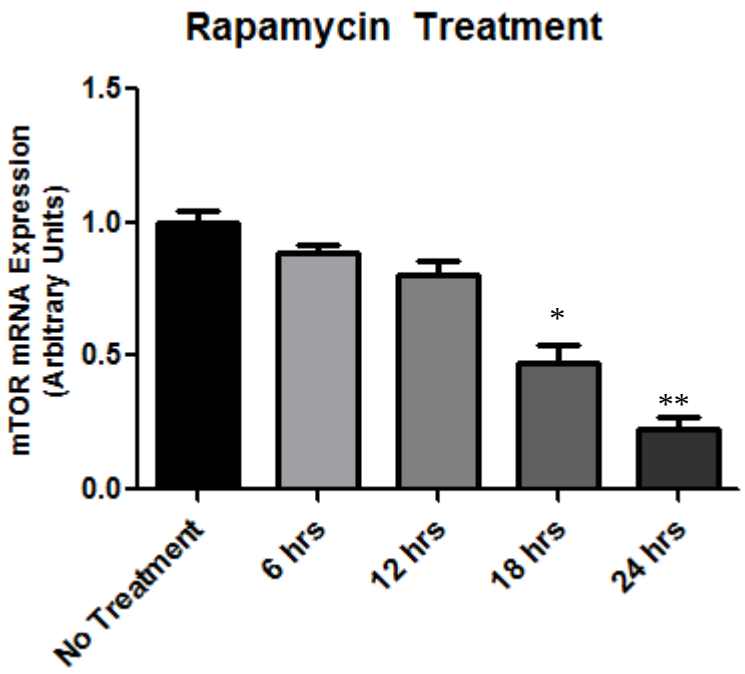

Figure 30. Assessment of mTOR in VSMCs treated with Rapamycin

Rapamycin-induced inhibition of mTOR in VSMCs over a 24 hour period causes a time dependent attenuation in mTOR mRNA expression levels by RT-qPCR analysis (n=3/group).

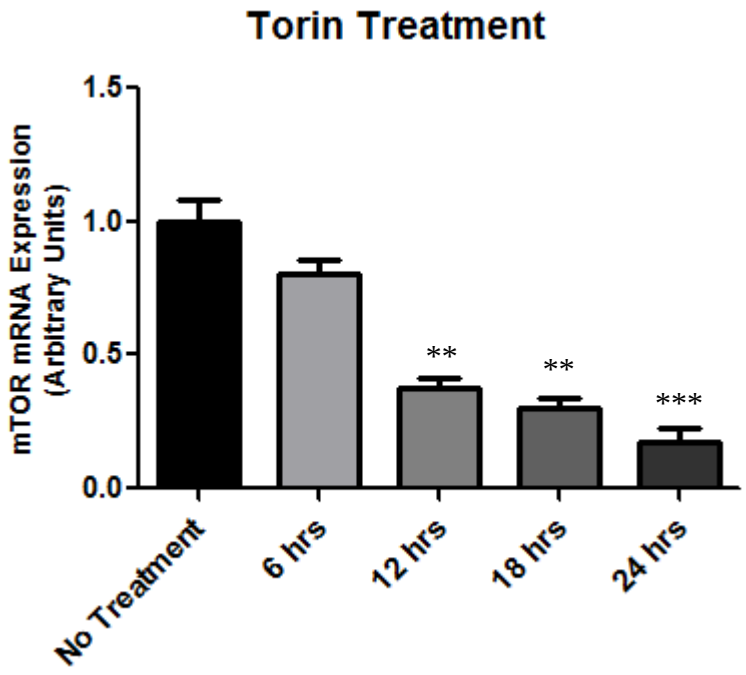

Figure 31. Assessment of mTOR in VSMCs treated with Torin.

Torin-induced inhibition of mTOR in VSMCs over a 24 hour period causes a time dependent reduction in mTOR mRNA expression levels by RT-qPCR analysis (n=3/group).

Attenuation of TET2 by mTOR

As previously shown, TET2 expression is negatively regulated via diet and genetic induced hyperlipidemia Thus, we next sought to assess the connection between TET2 and the mTOR pathway. To evaluate this pathway's role, VSMCs were treated with the mTOR inhibitors rapamycin and torin. After 24 hours treatment with mTOR inhibitor, TET2 levels in VSMCs were significantly elevated as compared with control untreated cells ($P<0.05$) (Figure 32). Furthermore, TET2 levels were more highly expressed with the more potent mTOR inhibitor, torin, as compared to treatment with rapamycin ($P<0,01$) (Figure 32).

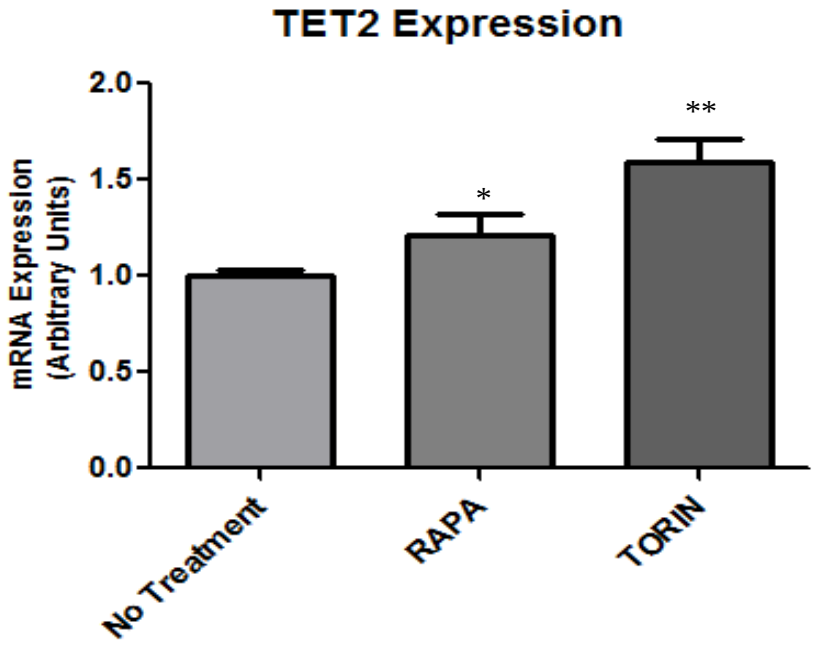

Figure 32. TET2 expression in VSMC treated with mTOR inhibitor

In response to inhibition of mTOR by rapamycin and torin, VSMCs treated for 24 hours show an increase in TET2 mRNA expression.

IGF-1R Expression in Response to Inhibition of mTOR.

Because rapamycin induces TET2 expression, we next sought to assess the connection between IGF-1R and rapamycin/torin-induced inhibition of the mTOR pathway. After 24 hours treatment with mTOR inhibitors ,IGF-1R levels in VSMCs were significantly elevated as compared with control untreated cells ($P<0.05$) (Figure 33).

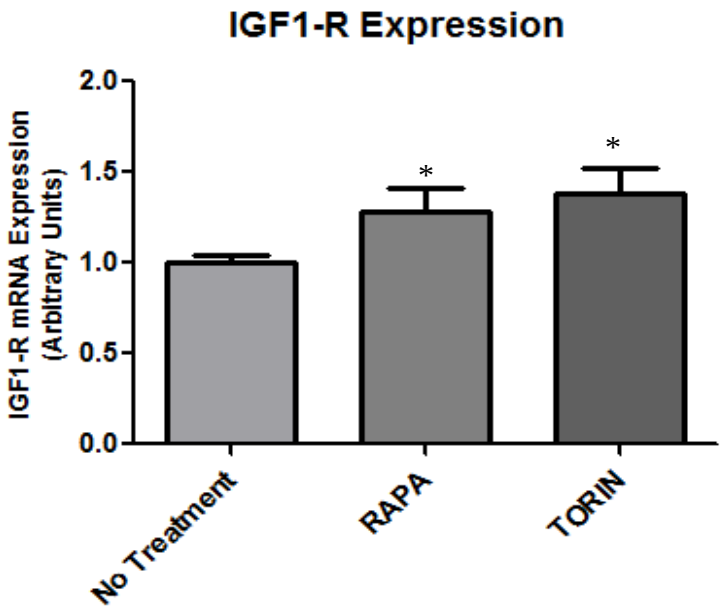

Figure 33. IGF-1R expression in VSMC treated with mTOR inhibitors.

Inhibition of mTOR by rapamycin and torin of VSMCs treated for 24 hours show an increase in IGF-1R mRNA expression ($P<0.05$) (n=3/group).

Chapter 5: Discussion

The Development of Atherosclerosis in Diet Adjusted and Genetically Modified Mice

In general, most rodent strains do not develop atherosclerosis as seen in humans and large animals (Zadelaar, Kleemann et al. 2007). However, the murine model provides one of the most frequently utilized and easily manipulated animal models for the study of atherosclerosis. Genetic manipulation through gene knockout and diet manipulation can both effectively and relatively quickly generate atherosclerotic plaque formation. We, as well as numerous others, have produced a murine model of atherosclerosis utilizing both diet-induced and genetically modified models. The combination of both diet-induced and/or the genetic knockout of the ApoE protein have allowed a wide spectrum of the disease with varying degrees of severity of atherosclerosis within the models.

To correlate the risk factors to epigenetic alterations in atherosclerosis, in this study we examined several basic physiological parameters in both wild type and ApoE knockout mice, including average body weight, BMI, hypertension, hypercholesterolemia, an cardiovascular function.

We observed significantly increased body weight and BMI in wild type mice fed a high fat diet. Additionally, ApoE knockout mice fed a high fat diet showed a higher average increase in weight and BMI. However, no significant difference in weight and BMI was found when comparing wild type and ApoE knockout groups without the diet-induced

weight gain. This is likely due to the fact that genetic knockout of the ApoE protein causes severe hypercholesterolemia with most of the plasma cholesterol within the VLDL fraction (Plump, Smith et al. 1992). However, the absence of ApoE also significantly impairs delivery of liver-derived VLDL to adipocytes. In the adipocytes, ApoE interacts with the VLDL receptor, which facilitates hydrolysis of triglycerides by lipoprotein lipases. Additionally, within the cells of atherosclerotic plaques the inability to secrete ApoE has been shown to have an independent proatherogenetic effect (Fazio, Babaev et al. 1997). This suggests that hyperlipidemia, whether through diet induction or ApoE knockout, is an essential prerequisite for atherosclerosis. However, as our results show, the induction of hyperlipidemia may not be associated with weight gain as reported with the ApoE knockout weight where the impaired delivery of liver-derived VLDL to adipocytes likely suppresses body weight gain and body fat accumulation.

Being closely related and a function of body weight, BMI, or body mass index, functionally quantifies the amount of tissue mass within the mouse. On normal chow, all groups fell within the normal BMI range. However, when subjected to a high fat diet, both wild type and ApoE knockout groups showed significant gains in BMI and were categorized as obese. Although obesity alone does not fully reveal the extent of atherosclerosis, it remains a significant risk factor and factors such as BMI and weight do positively correlate with the degree of atherosclerosis independent of other risk factors (Hubert, Feinleib et al. 1983).

Hypertension is a well-established cardiovascular risk factor that independently increases the risk of atherosclerosis (Alexander 1995). When subjected to a high fat diet, both wild type and ApoE deficient mice showed an increase in both systolic and diastolic

blood pressure over those groups fed a normal chow diet. Additionally, wild type mice fed a high fat diet showed blood pressure similar to that of ApoE knockout mice. Of the four groups, ApoE knockout mice fed a high fat diet showed the highest proclivity for hypertension with five of eight mice defined as hypertensive. Although not sufficient when taken alone, the elevated blood pressure in groups deficient for ApoE and those fed a high fat diet suggest a resulting increase in the amount and severity of atherosclerosis.

Ultrasound remains the most frequently used modality for the routine non-invasive evaluation of cardiac and vascular function in humans and experimental animals. Here we report that the degree of myocardial hypertrophy assessed by transthoracic echocardiography, as evidenced by LV wall thickness and IVS measurements, increased with genetic knockout of the ApoE protein. The degree of hypertrophy was further intensified with the addition of a high fat diet. We further demonstrate an aortic arch arterial wall thickening within the genetic knockout of ApoE that is progressively worsened by the addition of a high fat diet. Because of the nature and limitations of transthoracic aortic intimal wall evaluations, it is difficult to quantify the severity of atherosclerosis. Nevertheless, the morphological and functional characterization via ultrasound is consistent with myocardial hypertrophy and cardiovascular dysfunction caused by vascular occlusion associated with atherosclerosis.

The present study has identified, both qualitatively and quantitatively, intra-cytoplasmic neutral lipid accumulation within the aorta. *En face* Oil Red O staining in aortas demonstrated minimal lipid-rich atherosclerotic lesions within control wild type mice. However, in ApoE knockout mice these lesions become more numerous and larger, extending from the aortic outflow through the descending aorta. Overall lipid deposition

within the aortic arch increased with the addition of a high fat diet, while microscopic aortic ring analysis showed a progressive increase in cellular phenotypic dysfunction. Our data reveals an atherosclerotic progression from simple fatty streaks to fibroatheroma, displaying multiple lipid cores and fibrotic layers, in a model that is genetic knockout and diet inducible.

In this study, we generated a model for assessing the progression of atherosclerosis utilizing genetic and environmental factors. *In vivo* assessments of weight, blood pressure, echocardiography, and aortic ultrasound, as well as *ex vivo* examination and quantification of tissue reflect the pathophysiology. Our data, taken as a whole, shows varying degrees of severity of atherosclerosis within the models suitable for the assessment of the epigenetic contribution of DNA methylation and hydroxymethylation to the disease.

Global DNA Methylation and Hydroxymethylation in Diet Adjusted and Genetically Modified Mice Prone to Atherosclerosis.

There has been increasing experimental and clinical evidence supporting the concept that aberrant methylation patterns are present in cancerous and diseased states. Our data reveals a positive correlation between genome wide de-methylation and the severity of atherosclerosis. Additionally, we found a similar progressive loss in hydroxymethylation that was induced by both diet and genetic knockout of ApoE which closely correlated to the severity of atherosclerosis as determined by weight, blood pressure, echocardiography, and aortic ultrasound, as well as *ex vivo* examination. These findings suggest that methylation and hydroxymethylation could influence the onset and progression of arthrosclerosis

because of their capacity to affect gene expression and their alteration in response to genetic and environmental influences such as diet. Furthermore, our finding lends itself to further investigation of the role of DNA methylation and hydroxymethylation during the development of arthrosclerosis.

Locus Specific DNA Methylation and Hydroxymethylation.

Within the selection of genes tested we report significant differences in the level of hydroxymethylation in normal and advanced atherosclerotic tissue. Of the genes tested for the presence of 5-hydroxymethylcytosine, IGF-1R showed significant differences during atherosclerotic progression, which may be an indication of its sensitivity to, and regulation by, epigenetic control. We report the reduction of the mRNA transcript and protein level of IGF-1R associated with the severity of atherosclerosis. The correlation between increases in epigenetic marks 5-methylcytosine and the decrease in 5-hydroxymethylcytosine along with the reduction of IGF-1R through atherogenesis suggest the presence of a mechanism of epigenetic regulation of IGF-1R.

TET Methylcytosine Dioxygenase Family of Enzymes in Atherosclerosis.

The conversion of the base 5-methylcytosine to 5-hydroxymethylcytosine is governed by the TET methylcytosine dioxygenase family of enzymes. Our data reveals negligible levels of TET1 and TET3 within the aortic vasculature and VSMCs during normal physiology. The presence of both 5-hydroxymethylcytosine and TET2 within the

aortic vasculature and VSMCs suggests that TET2 is the sole modulator of this conversion. Furthermore, the data reveals that TET2 is attenuated during the onset and progression of atherosclerosis. This reduction is positively correlated with the degree of atherosclerosis and, additionally, its attenuation is consistent with the reductions in the level of hydroxymethylation within the IGF-1R promoter region. The findings that TET2 is the sole modulator of this conversion and is affected by the degree of atherosclerosis reveals a novel epigenetic regulation of vascular cell signal transduction and proliferation during atherosclerosis. It suggests that during normal physiology TET2 plays a role in the regulation of the balance between DNA hydroxymethylation and methylation, and to that end, activation and inactivation of IGF-1R expression during atherosclerosis.

Potential Targets of Rapamycin (mTOR) for Epigenetics of Atherosclerosis.

Mechanistic target of rapamycin (mTOR) is a master regulator of cell growth, proliferation, motility, survival, protein synthesis, autophagy, and transcription. The complex mTORC1 acts as a nutrient/energy/redox sensor and controls protein synthesis, becoming active in the presence of increased cellular nutrient, oxygen, and energy levels (Weichhart 2012). Consistent with other reports, we find that mTOR mRNA transcript and protein level are up-regulated by the addition of a high fat diet. This increase is also seen within the hypercholesterolemic ApoE knockout model, which is further up-regulated within this model with the addition of a high fat diet. The mTOR pathway, in addition to its role in nutrient sensing, cell growth, and proliferation, has been shown to be a regulator of SMC differentiation (Martin, Rzucidlo et al. 2004). Through rapamycin-induced inhibition of the

mTOR pathway, our data indicates that TET2 is negatively attenuated by diet induced up-regulation of mTOR. Moreover, when mTORC1 is inhibited via rapamycin, TET2 levels are up-regulated and our data shows downstream levels of 5-hydroxymethylcytosine are increased within the promoter of IGF-1R. Accompanying the increased levels of 5-hydroxymethylcytosine within the promoter region of IGF-1R, we also report the reactivation of IGF-1R expression through increases in IGF-1R mRNA transcript levels.

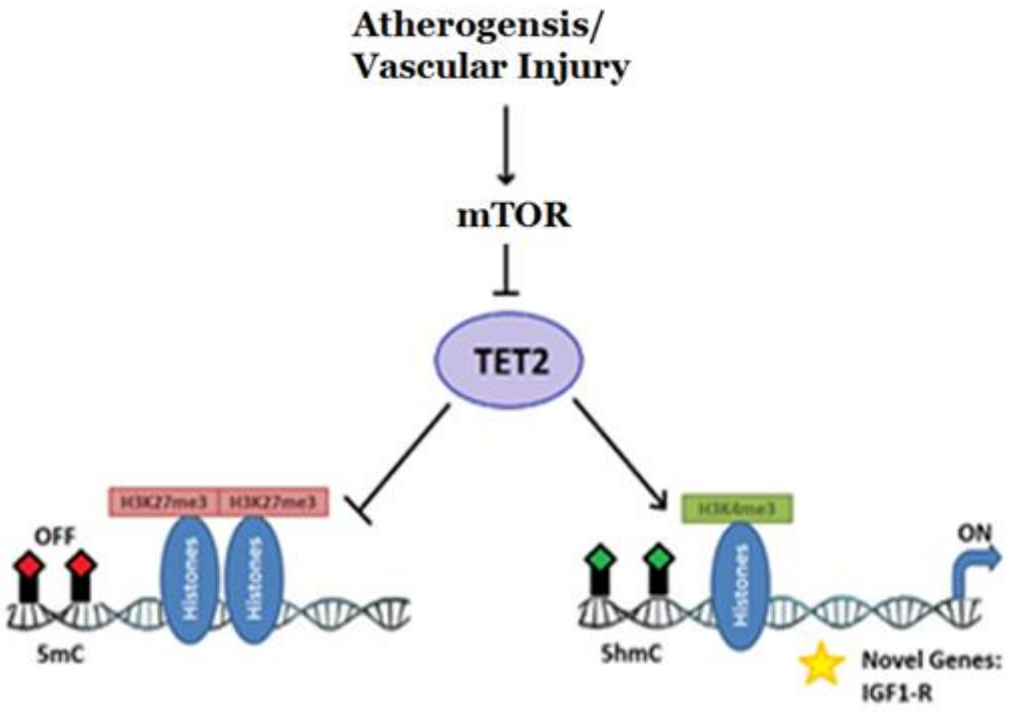

Figure 34. Schematic Representation of a Potential Mechanism of IGF-1R Gene Regulation Via DNA Hydroxymethylation.

Atherogenesis induced via genetic knockout of ApoE or diet up-regulates the mTOR pathway which in turn negatively regulates TET2. CpG rich loci within IGF-1R have been implicated in the binding of TET2 which then catalyzes the conversion of 5-methylcytosine to 5-hydroxymethylcytosine, an activator of gene expression.

Conclusions

Previous reports have indicated a link between mTOR and IGF-1 signaling (Johnson, Rabinovitch et al. 2013). During normal cell function IGF-1R signaling via insulin receptor substrate 1/2 (IRS 1/2) activates the PI3K/AKT pathway. IRS 1/2, through direct and indirect down-stream targets, blocks negative cell functions such as oxidative stress, apoptosis, pro-inflammatory signaling, and cellular dysfunction while mTOR, through activation of the IRS 1/2/PI3K/Akt pathway causes cell growth, survival, and protein synthesis. However, mTOR pathway activation via cellular nutrients and energy, as well as, IGF-1R signaling changes during overstimulation. Excessive activation of the mTOR/S6K pathway creates a negative feedback loop and inactivates IRS1/2, thus causing insulin and IGF-1R signaling resistance (Blagosklonny 2013). In this way, IGF-1R exerts its effect on mTOR signaling with the possibility of attenuation during excessive activation or overstimulation. Our novel finding that vascular cell signal transduction and proliferation though IGF-1R can be up-regulated via rapamycin-induced inhibition of the mTOR pathway creates an additional level of regulation via overstimulation of mTOR leading to down-regulation of TET2, and thus, down-regulation of IGF-1R via loss of 5-hydroxymethylcytosine.

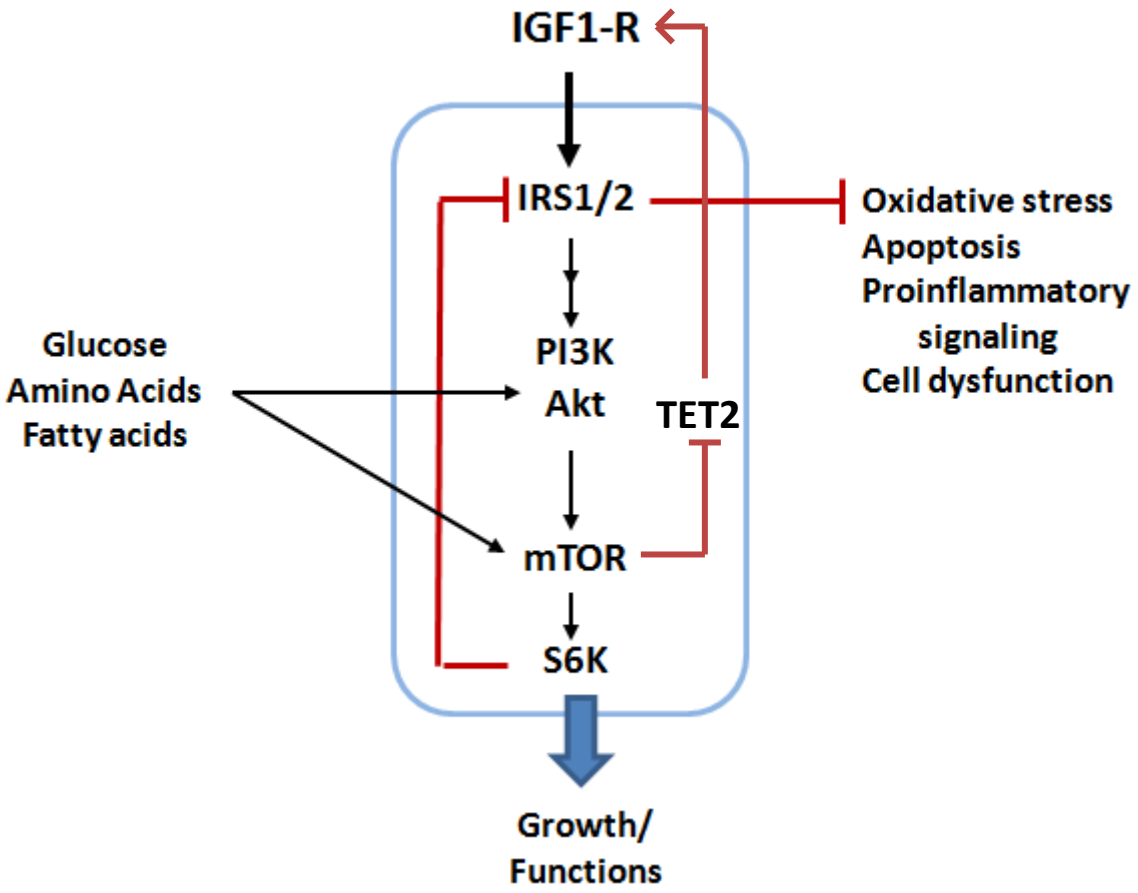

Figure 35. Schematic Representation of the Potential Epigenetic Regulation of IGF-1R Expression and Signaling.

IGF-1Rsignaling via insulin receptor substrate 1/2 (IRS1/2) activates the PI3K/Akt/mTOR/S6K pathway. The mTOR/S6K pathway is also activated by nutrients such as glucose, TNF and numerous other factors. Excessive activation of mTOR/S6K pathway in turn inactivates IRS1/2, thus causing insulin resistance.

The mTOR pathway has been a target for many years because of its implication in restenosis. Rapamycin has be used within intra arterial stents to prevent arterial intimal thickening and numerous studies have shown rapamycin prevents proliferation of not only T cells but also proliferation and migration of VSMCs (Mohacsi, Tuller et al. 1997). Several pathways have been implicated for rapamycin's affect including blocking G1/S transition by binding to a cytosolic receptor, FK506 binding protein 12. Rapamycin binding to FK506BP12 ultimately prevents proliferation by reducing cdk2 activity (Marx, Jayaraman et al. 1995). Here we report an additional pathway in which rapamycin/mTOR/TET2 could affect VSMC contractility, metabolism, hypertrophy, apoptosis, autophagy, stem cell regeneration and senescence through the known effects of IGF-1R function (Ren and Anversa 2015).

Further studies

The novel finding that the normal vascular cell signaling of IGF-1R during atherosclerosis can be epigenetically up-regulated via rapamycin-induced inhibition of the mTOR pathway leads to the possibility of clinical intervention. In the case of atherosclerosis, the possibility exists of utilizing this pathway to restore normal cellular function. An example of which would be the utilization of a combinatory rapamycin and TET2 eluting stent which may present a possible novel avenue of investigation to combat restenosis and restore normal function. Further investigation may also lead to advancements in oncology. Aberrant IGF-1 signaling is indicated in, and a hallmark of, a host of cancers. Rhabdomyosarcomas (RMSs) are the most common soft tissue sarcomas of childhood and

adolescence. RMSs as well as numerous other cancers exploit the IGF-1R pathway. In RMSs, rapamycin is frequently used as an anti-proliferative cancer treatment through its inhibition of mTOR downstream signaling. Paradoxically, treatment of cancer cells with rapamycin activates AKT, due to blockade of the previously mentioned feedback loop via (S6K). Through dual treatment of RMS tumors with rapamycin and TET2 inhibitors the proliferative IGF-1R signaling cascade may be dramatically reduced. In this way, the mTOR/TET2/IGF-1R pathway may become an attractive possible treatment for not only RMSs, but other IGF-1R driven cancers and numerous disease conditions in which aberrant IGF-1R signaling is indicated

References

(2015). "Global, regional, and national age-sex specific all-cause and cause-specific mortality for 240 causes of death, 1990-2013: a systematic analysis for the Global Burden of Disease Study 2013." Lancet 385(9963): 117-171.

Alexander, R. W. (1995). "Theodore Cooper Memorial Lecture. Hypertension and the pathogenesis of atherosclerosis. Oxidative stress and the mediation of arterial inflammatory response: a new perspective." Hypertension 25(2): 155-161.

Arber, W. and D. Dussoix (1962). "Host specificity of DNA produced by Escherichia coli. I. Host controlled modification of bacteriophage lambda." J Mol Biol 5: 18-36.

Beisiegel, U., W. Weber, et al. (1988). "Apolipoprotein E-binding proteins isolated from dog and human liver." Arteriosclerosis 8(3): 288-297.

Blagosklonny, M. V. (2013). "TOR-centric view on insulin resistance and diabetic complications: perspective for endocrinologists and gerontologists." Cell Death Dis 4: e964.

Brown, E. J., M. W. Albers, et al. (1994). "A mammalian protein targeted by G1-arresting rapamycin-receptor complex." Nature 369(6483): 756-758.

Castro, R., I. Rivera, et al. (2003). "Increased homocysteine and S-adenosylhomocysteine concentrations and DNA hypomethylation in vascular disease." Clin Chem 49(8): 1292-1296.

Cedazo-Minguez, A. (2007). "Apolipoprotein E and Alzheimer's disease: molecular mechanisms and therapeutic opportunities." J Cell Mol Med 11(6): 1227-1238.

Chen, T., Y. Ueda, et al. (2003). "Establishment and maintenance of genomic methylation patterns in mouse embryonic stem cells by Dnmt3a and Dnmt3b." Mol Cell Biol 23(16): 5594-5605.

Choy, M. K., M. Movassagh, et al. (2010). "Genome-wide conserved consensus transcription factor binding motifs are hyper-methylated." BMC Genomics 11: 519.

Dawber, T. R., G. F. Meadors, et al. (1951). "Epidemiological approaches to heart disease: the Framingham Study." Am J Public Health Nations Health 41(3): 279-281.

Dong, C., W. Yoon, et al. (2002). "DNA methylation and atherosclerosis." J Nutr 132(8 Suppl): 2406S-2409S.

Dutta, P., G. Courties, et al. (2012). "Myocardial infarction accelerates atherosclerosis." Nature 487(7407): 325-329.

Dzau, V. J. (1988). "Mechanism of the interaction of hypertension and hypercholesterolemia in atherogenesis: the effects of antihypertensive agents." Am Heart J 116(6 Pt 2): 1725-1728.

Ehrlich, M., M. A. Gama-Sosa, et al. (1982). "Amount and distribution of 5-methylcytosine in human DNA from different types of tissues of cells." Nucleic Acids Res 10(8): 2709-2721.

Fang, Y., M. Vilella-Bach, et al. (2001). "Phosphatidic acid-mediated mitogenic activation of mTOR signaling." Science 294(5548): 1942-1945.

Fazio, S., V. R. Babaev, et al. (1997). "Increased atherosclerosis in mice reconstituted with apolipoprotein E null macrophages." Proc Natl Acad Sci U S A 94(9): 4647-4652.

Frias, M. A., C. C. Thoreen, et al. (2006). "mSin1 is necessary for Akt/PKB phosphorylation, and its isoforms define three distinct mTORC2s." Curr Biol 16(18): 1865-1870.

Frommer, M., L. E. McDonald, et al. (1992). "A genomic sequencing protocol that yields a positive display of 5-methylcytosine residues in individual DNA strands." Proc Natl Acad Sci U S A 89(5): 1827-1831.

Globisch, D., M. Munzel, et al. (2010). "Tissue distribution of 5-hydroxymethylcytosine and search for active demethylation intermediates." PLoS One 5(12): e15367.

Go, A. S., D. Mozaffarian, et al. (2014). "Heart disease and stroke statistics--2014 update: a report from the American Heart Association." Circulation 129(3): e28-e292.

Guo, J. U., Y. Su, et al. (2011). "Hydroxylation of 5-methylcytosine by TET1 promotes active DNA demethylation in the adult brain." Cell 145(3): 423-434.

Hata, K., M. Okano, et al. (2002). "Dnmt3L cooperates with the Dnmt3 family of de novo DNA methyltransferases to establish maternal imprints in mice." Development 129(8): 1983-1993.

Hay, N. and N. Sonenberg (2004). "Upstream and downstream of mTOR." Genes Dev 18(16): 1926-1945.

He, Y. F., B. Z. Li, et al. (2011). "Tet-mediated formation of 5-carboxylcytosine and its excision by TDG in mammalian DNA." Science 333(6047): 1303-1307.

Helliwell, S. B., P. Wagner, et al. (1994). "TOR1 and TOR2 are structurally and functionally similar but not identical phosphatidylinositol kinase homologues in yeast." Mol Biol Cell 5(1): 105-118.

Holliday, R. (1994). "Epigenetics: an overview." Dev Genet 15(6): 453-457.

Hsieh, C. L. (1999). "Evidence that protein binding specifies sites of DNA demethylation." Mol Cell Biol 19(1): 46-56.

Hubert, H. B., M. Feinleib, et al. (1983). "Obesity as an independent risk factor for cardiovascular disease: a 26-year follow-up of participants in the Framingham Heart Study." Circulation 67(5): 968-977.

Johnson, S. C., P. S. Rabinovitch, et al. (2013). "mTOR is a key modulator of ageing and age-related disease." Nature 493(7432): 338-345.

Jones, P. A. (2012). "Functions of DNA methylation: islands, start sites, gene bodies and beyond." Nat Rev Genet 13(7): 484-492.

Kim, D. H., D. D. Sarbassov, et al. (2002). "mTOR interacts with raptor to form a nutrient-sensitive complex that signals to the cell growth machinery." Cell 110(2): 163-175.

Kim, D. H., D. D. Sarbassov, et al. (2003). "GbetaL, a positive regulator of the rapamycin-sensitive pathway required for the nutrient-sensitive interaction between raptor and mTOR." Mol Cell 11(4): 895-904.

Kimura, H. and K. Shiota (2003). "Methyl-CpG-binding protein, MeCP2, is a target molecule for maintenance DNA methyltransferase, Dnmt1." J Biol Chem 278(7): 4806-4812.

Koo, C., M. E. Wernette-Hammond, et al. (1988). "Uptake of cholesterol-rich remnant lipoproteins by human monocyte-derived macrophages is mediated by low density lipoprotein receptors." J Clin Invest 81(5): 1332-1340.

Kunz, J., R. Henriquez, et al. (1993). "Target of rapamycin in yeast, TOR2, is an essential phosphatidylinositol kinase homolog required for G1 progression." Cell 73(3): 585-596.

Libby, P. (2002). "Inflammation in atherosclerosis." Nature 420(6917): 868-874.

Martin, K. A., E. M. Rzucidlo, et al. (2004). "The mTOR/p70 S6K1 pathway regulates vascular smooth muscle cell differentiation." Am J Physiol Cell Physiol 286(3): C507-517.

Marx, S. O., T. Jayaraman, et al. (1995). "Rapamycin-FKBP inhibits cell cycle regulators of proliferation in vascular smooth muscle cells." Circ Res 76(3): 412-417.

Mohacsi, P. J., D. Tuller, et al. (1997). "Different inhibitory effects of immunosuppressive drugs on human and rat aortic smooth muscle and endothelial cell proliferation stimulated by platelet-derived growth factor or endothelial cell growth factor." J Heart Lung Transplant 16(5): 484-492.

Montenegro, M. R. and L. A. Solberg (1968). "Obesity, body weight, body length, and atherosclerosis." Lab Invest 18(5): 594-603.

Mozaffarian, D., E. J. Benjamin, et al. (2015). "Heart disease and stroke statistics--2015 update: a report from the American Heart Association." Circulation 131(4): e29-322.

Nan, X., R. R. Meehan, et al. (1993). "Dissection of the methyl-CpG binding domain from the chromosomal protein MeCP2." Nucleic Acids Res 21(21): 4886-4892.

Nan, X., H. H. Ng, et al. (1998). "Transcriptional repression by the methyl-CpG-binding protein MeCP2 involves a histone deacetylase complex." Nature 393(6683): 386-389.

Okano, M., D. W. Bell, et al. (1999). "DNA methyltransferases Dnmt3a and Dnmt3b are essential for de novo methylation and mammalian development." Cell 99(3): 247-257.

Paigen, B., A. Morrow, et al. (1987). "Quantitative assessment of atherosclerotic lesions in mice." Atherosclerosis 68(3): 231-240.

Plump, A. S., J. D. Smith, et al. (1992). "Severe hypercholesterolemia and atherosclerosis in apolipoprotein E-deficient mice created by homologous recombination in ES cells." Cell 71(2): 343-353.

Post, W. S., P. J. Goldschmidt-Clermont, et al. (1999). "Methylation of the estrogen receptor gene is associated with aging and atherosclerosis in the cardiovascular system." Cardiovasc Res 43(4): 985-991.

Price, A. E. (2004). "Heart disease and work." Heart 90(9): 1077-1084.

Rader, D. J. and A. Daugherty (2008). "Translating molecular discoveries into new therapies for atherosclerosis." Nature 451(7181): 904-913.

Ramsahoye, B. H., D. Biniszkiewicz, et al. (2000). "Non-CpG methylation is prevalent in embryonic stem cells and may be mediated by DNA methyltransferase 3a." Proc Natl Acad Sci U S A 97(10): 5237-5242.

Ren, J. and P. Anversa (2015). "The insulin-like growth factor I system: physiological and pathophysiological implication in cardiovascular diseases associated with metabolic syndrome." Biochem Pharmacol 93(4): 409-417.

Sarbassov, D. D., S. M. Ali, et al. (2004). "Rictor, a novel binding partner of mTOR, defines a rapamycin-insensitive and raptor-independent pathway that regulates the cytoskeleton." Curr Biol 14(14): 1296-1302.

Schubeler, D. (2015). "Function and information content of DNA methylation." Nature 517(7534): 321-326.

Selwyn, A. P., S. Kinlay, et al. (1997). "Atherogenic lipids, vascular dysfunction, and clinical signs of ischemic heart disease." Circulation 95(1): 5-7.

Sharif, J., M. Muto, et al. (2007). "The SRA protein Np95 mediates epigenetic inheritance by recruiting Dnmt1 to methylated DNA." Nature 450(7171): 908-912.

Singh, V., R. L. Tiwari, et al. (2009). "Models to study atherosclerosis: a mechanistic insight." Curr Vasc Pharmacol 7(1): 75-109.

Stein, R., A. Razin, et al. (1982). "In vitro methylation of the hamster adenine phosphoribosyltransferase gene inhibits its expression in mouse L cells." Proc Natl Acad Sci U S A 79(11): 3418-3422.

Svenson KL, F. J., Donahue L, Paigen B. (2015) "Bone mineral density and body composition in C57BL/6J-Chr#PWD/Ph/ForeJ mouse chromosome substitution strains. ." Mouse Phenome Database web site, The Jackson Laboratory, Bar Harbor, Maine USA. .

Tahiliani, M., K. P. Koh, et al. (2009). "Conversion of 5-methylcytosine to 5-hydroxymethylcytosine in mammalian DNA by MLL partner TET1." Science 324(5929): 930-935.

Vardimon, L., A. Kressmann, et al. (1982). "Expression of a cloned adenovirus gene is inhibited by in vitro methylation." Proc Natl Acad Sci U S A 79(4): 1073-1077.

Weichhart, T. (2012). mTor : methods and protocols. New York, Humana Press.

Wion, D. and J. Casadesus (2006). "N6-methyl-adenine: an epigenetic signal for DNA-protein interactions." Nat Rev Microbiol 4(3): 183-192.

Wossidlo, M., T. Nakamura, et al. (2011). "5-Hydroxymethylcytosine in the mammalian zygote is linked with epigenetic reprogramming." Nat Commun 2: 241.

Zadelaar, S., R. Kleemann, et al. (2007). "Mouse models for atherosclerosis and pharmaceutical modifiers." Arterioscler Thromb Vasc Biol 27(8): 1706-1721.

. Vita

Jason Williams was born in Newport, New Hampshire on April 9, 1986, the son of Cindy Williams and Mark Williams. After completing junior year of high school at Newport High School, Newport NH he attended Clarkson University, Potsdam NY. He entered Baylor University in 2004 and received the degree of Bachelor of Arts with a major in biology in 2008. The following year he worked as a research associate the Department of Stem Cell Biology at The University of Texas Institute of Molecular Medicine. In September of 2009 he entered The University of Texas Graduate School of Biomedical Sciences at Houston

Permanent address:

8300 El Mundo St. Apt. 209

Houston, Texas 77054